

THE BLOCK-POISSON ESTIMATOR FOR OPTIMALLY TUNED EXACT SUBSAMPLING MCMC

MATIAS QUIROZ^{1,2}, MINH-NGOC TRAN³, MATTIAS VILLANI^{4,5},
ROBERT KOHN⁶ AND KHUE-DUNG DANG¹

ABSTRACT. Speeding up Markov Chain Monte Carlo (MCMC) for datasets with many observations by data subsampling has recently received considerable attention. A pseudo-marginal MCMC method is proposed that estimates the likelihood by data subsampling using a block-Poisson estimator. The estimator is a product of Poisson estimators, allowing us to update a single block of subsample indicators in each MCMC iteration so that a desired correlation is achieved between the logs of successive likelihood estimates. This is important since pseudo-marginal MCMC with positively correlated likelihood estimates can use substantially smaller subsamples without adversely affecting the sampling efficiency. The block-Poisson estimator is unbiased but not necessarily positive, so the algorithm runs the MCMC on the absolute value of the likelihood estimator and uses an importance sampling correction to obtain consistent estimates of the posterior mean of any function of the parameters. Our article derives guidelines to select the optimal tuning parameters for our method and shows that it compares very favourably to regular MCMC without subsampling, and to two other recently proposed exact subsampling approaches in the literature.

KEYWORDS: Bayesian inference, Control variates, Data subsampling, Exact inference, Poisson Estimator, Pseudo-marginal MCMC.

1. INTRODUCTION

Standard Markov Chain Monte Carlo (MCMC) algorithms for Bayesian inference require a large number of likelihood function evaluations and are therefore prohibitively expensive for datasets with many observations. This is a real obstacle for industrial applications where huge amounts are recorded using modern sensor technology, and in the natural and

¹*School of Mathematical and Physical Sciences, University of Technology Sydney.* ²*Research Division, Sveriges Riksbank.* ³*Discipline of Business Analytics, University of Sydney.* ⁴*Department of Statistics, Stockholm University.* ⁵*Department of Computer and Information Science, Linköping University.* ⁶*School of Economics, UNSW Business School, University of New South Wales.*

social sciences where datasets are increasingly larger; digitalization is also turning text into data and also the humanities are now concerned with big data. A recent literature therefore attempts to speed up MCMC algorithms by using random subsets of the data; see Korattikara et al. (2014); Bardenet et al. (2014, 2017); Maclaurin and Adams (2014); Quiroz et al. (2019, 2018b) and Bierkens et al. (2019). Section 2 briefly reviews these approaches and highlights possible pitfalls.

Bardenet et al. (2017) provide an excellent review of subsampling approaches and propose a positive unbiased estimator of the likelihood in a pseudo-marginal framework (Andrieu and Roberts, 2009) to accelerate the Metropolis-Hastings (MH) algorithm (Metropolis et al., 1953; Hastings, 1970). Their unbiased likelihood estimator is constructed from a sequence of unbiased log-likelihood estimates from small batches of observations used in a Rhee-Glynn type debiasing estimator (Rhee and Glynn, 2015). To ensure positiveness, Bardenet et al. (2017) use a lower bound for the log-likelihood estimates in all batches (Jacob and Thiery, 2015), but they find that the large variability of their estimator causes the chain to mix poorly.

We propose an alternative unbiased estimator of the likelihood having several attractive properties and demonstrate that it can be successfully used for subsampling MCMC. This block-Poisson estimator is a product of Poisson estimators (Wagner 1988; Papaspiliopoulos, 2009), where each estimator is based on a block of observations. Our estimator has the following four key features. First, the product form makes it possible to only update the subsamples in some of the blocks in each iteration to target a given correlation between the logs of the estimated likelihood at the current and proposed MH draws. Deligiannidis et al. (2018) show that such dependent pseudo-marginal schemes are very efficient because they can use substantially noisier likelihood, and hence smaller subsamples, without adversely affecting the sampling efficiency of the chain. Our blocking strategy makes it possible to directly control the correlation, and to update the subsample without proposing moves for all the subsample indicators in the dataset. Second, the block-Poisson estimator has a lower variance than the Rhee-Glynn estimator in Bardenet et al. (2017). Third, the block-Poisson

estimator uses variance reducing control variates proposed in Bardenet et al. (2017) and Quiroz et al. (2019). Fourth, the block-Poisson estimator uses a soft lower bound for its constituent batch estimators, rather than a strict lower bound as in Bardenet et al. (2017). Section 3.3 explains why a soft lower bound is computationally more efficient than a strict bound. However, the soft bound makes it possible to obtain negative likelihood estimates, which cannot be used within the usual pseudo-marginal MCMC framework in Andrieu and Roberts (2009). Lyne et al. (2015) propose an ingenious solution to the problem of negative likelihood estimates by running the pseudo-marginal sampler on the absolute value of the likelihood estimate followed by an importance sampling correction step to estimate the posterior mean of any function of the model parameters. We refer to this pseudo-marginal Metropolis-Hastings with importance sampling sign correction as *signed PMMH*.

It is well known that pseudo-marginal algorithms need to carefully tune the number of particles (subsamples) and several recent papers develop practical guidelines for this choice for strictly positive likelihood estimators; see Pitt et al. (2012), Doucet et al. (2015) and Sherlock et al. (2015). A major contribution of our article is the derivation of easily implemented guidelines for the optimal number of subsamples (or more generally particles) for the signed PMMH based on the block-Poisson estimator. The optimal number of subsamples is chosen to minimize the asymptotic variance of the importance sampling estimator for a given computational budget and therefore balances: i) the inefficiency in the MCMC on the absolute measure, ii) the computational cost of the likelihood estimator and iii) the probability of negative estimates in signed PMMH. We show that the asymptotic variance of the importance sampling estimator can be obtained in closed form when the likelihood is estimated by the block-Poisson estimator. The guidelines are derived under idealized conditions, but are demonstrated to be quite accurate in empirical experiments. The proposed framework to derive these optimality results applies more generally than subsampling; for example it can be applied to doubly intractable problems using the Exponential auxiliary variable construction in Lyne et al. (2015).

Our article demonstrates that subsampling MCMC using the block-Poisson estimator is an efficient sampler that mixes well and is more efficient than a MH sampler on the full sample. It also shows empirically that our exact subsampling MCMC is much more efficient than Firefly Monte Carlo (Maclaurin and Adams, 2014), a highly cited exact subsampling algorithm. We also show empirically that our approach scales better with respect to the dimension of the parameter space than the zig-zag sampler in Bierkens et al. (2019). Our approach is also fully automatic without requiring manual derivations of model specific upper bounds; see Section 5.4.

The rest of the article is organized as follows. Section 2 briefly reviews the main subsampling approaches proposed in the recent literature. Section 3 introduces the block-Poisson estimator and derives its key properties. Section 4 outlines the proposed sampling algorithm and provides guidelines on the selection of tuning parameters to obtain an optimal implementation. Section 5 demonstrates the methodology and Section 6 concludes. The paper has an online supplement containing proofs, additional material and extensions. We refer to equations, sections, lemmas in the main paper as (1), Section 1, Lemma 1 etc., and to equations, sections and lemmas, etc in the supplement as (S1), Section S1 and Lemma S1, etc.

2. PREVIOUS RESEARCH

Previous research in scalable MCMC by data subsampling is either approximate (e.g. Korattikara et al., 2014; Bardenet et al., 2014, 2017; Quiroz et al., 2019) or exact (e.g. Maclaurin and Adams, 2014; Bierkens et al., 2019). Banterle et al. (2019), Payne and Mallick (2018) and Quiroz et al. (2018a) propose using delayed acceptance MCMC where the acceptance probability in the first stage is computed from on a subsample. However, the second stage is computed on the full sample and therefore the methods are not fully subsampling approaches.

The algorithms in Korattikara et al. (2014) and Bardenet et al. (2014, 2017) replace the computationally costly MH ratio with a hypothesis test based on a fraction of the data; Bardenet et al. (2017) and Quiroz et al. (2019) evaluate these methods.

Quiroz et al. (2019) estimate the MH ratio based on a random subsample of the data and use a dependent pseudo-marginal approach to sample from the posterior. They derive an efficient unbiased log-likelihood estimator with control variates and apply an approximate bias-correction to get an *approximately* unbiased likelihood estimator. Their target MCMC distribution is a perturbation of the posterior which they show is within $O(n^{-1}m^{-2})$ of the true posterior, where n is the sample size and m the subsample size. However, their bias-correction implies that the approximation error is a function of the variance of the log-likelihood estimator, and targeting a large variance may therefore degrade the posterior approximation. The approximation error is small in their examples even when the variance of the log-likelihood estimator is large, but there is no guarantee that this will hold in other applications. In contrast, our proposed method is exact in the sense that it provides simulation consistent estimates of posterior expectation of any function of the parameters, regardless of the estimator’s variability. See Section S4 of the supplement for a comparison with the approximate approach in Quiroz et al. (2019).

The Firefly Monte Carlo algorithm in Maclaurin and Adams (2014) introduces an auxiliary variable for each observation which determines if it should be included in the evaluation of the posterior in a given MCMC iteration. A lower bound for each likelihood term caters for the excluded observations. The authors suggest using Gibbs sampling with the original parameters and the auxiliary variables in two different blocks. The method has been documented to be very inefficient; see e.g. Bardenet et al. (2017); Li et al. (2020); Quiroz et al. (2019).

The zig-zag sampler (Bierkens et al., 2019) and the bouncy particle sampler (Bouchard-Côté et al., 2018) are two recent exact non-reversible subsampling MCMC algorithms based on piecewise deterministic Markov processes. While the samples from the zig-zag and bouncy

particle algorithms converge in distribution to the posterior, our method only gives simulation consistent estimates of the posterior mean of functions of the parameters. Section 5.4 compares our approach with the zig-zag sampler.

3. THE BLOCK-POISSON ESTIMATOR

3.1. The estimator and its properties. Suppose that the observations $y := (y_1 \dots, y_n)$ are conditionally independent given a parameter vector $\theta \in \Theta \subset \mathbb{R}^p$. The likelihood can then be written as

$$(3.1) \quad L(\theta) := p(y|\theta) = \exp(\ell(\theta)), \quad \ell(\theta) = \sum_{k=1}^n \ell_k(\theta), \quad \text{where } \ell_k(\theta) := \log p(y_k|\theta, x_k)$$

is the log-likelihood contribution of the k th observation with covariates x_k . Our method can also be used for longitudinal data where subjects are subsampled instead of individual observations. It also applies to stationary time series data by subsampling in the frequency domain; see Salomone et al. (2020).

The block-Poisson estimator of the likelihood in Definition 1 below relies on an unbiased estimator of the log-likelihood, $\ell(\theta)$. Quiroz et al. (2019) propose estimating $\ell(\theta)$ by a *difference estimator* based on computationally efficient control variates. The control variate $q_k(\theta)$ for the k th observation is such that the difference $d_k(\theta) = \ell_k(\theta) - q_k(\theta)$ is small. The difference estimator uses the equation

$$(3.2) \quad \ell(\theta) = q(\theta) + d(\theta), \quad \text{where } q(\theta) = \sum_{k=1}^n q_k(\theta) \quad \text{and} \quad d(\theta) = \sum_{k=1}^n d_k(\theta)$$

to estimate $\ell(\theta)$ by unbiasedly estimating $d(\theta)$. Since the control variates capture the size of each $\ell_k(\theta)$, it is efficient to use a simple sample mean estimator from a subsample of size m drawn with replacement to estimate d as

$$(3.3) \quad \hat{d}_m = \frac{n}{m} \sum_{i=1}^m d_{u_i},$$

where the u_i are iid from the distribution $\Pr(u_i = k) = 1/n$ for $k = 1, \dots, n$, and we suppress the dependence on θ to simplify notation. The variance of the difference estimator is

$$\sigma_{\hat{d}}^2 := V[\hat{d}_m] = \frac{\gamma}{m}, \text{ where } \gamma := n^2 \sigma_{d_{u_i}}^2 \text{ with } \sigma_{d_{u_i}}^2 := V[d_{u_i}].$$

There are several proposals for unbiasedly estimating the likelihood in the literature; see e.g. the Rhee-Glynn estimator (Rhee and Glynn, 2015), Russian roulette estimators (Lyne et al., 2015) and the Poisson estimator (Wagner, 1988). We now propose a modified Poisson estimator which is constructed to be particularly useful for the block pseudo-marginal algorithm developed in Section 4.

Definition 1. *The block-Poisson likelihood estimator is defined as*

$$(3.4) \quad \hat{L}_B(\theta) := \exp(q(\theta)) \prod_{l=1}^{\lambda} \xi_l, \text{ where } \xi_l = \exp\left(\frac{a + \lambda}{\lambda}\right) \prod_{h=1}^{\mathcal{X}_l} \left(\frac{\hat{d}_m^{(h,l)} - a}{\lambda}\right),$$

where λ is a positive integer, a is a real number, $\hat{d}_m^{(h,l)}$ is some unbiased estimator of $d = \ell - q$ from a small batch of m observations, and $\mathcal{X}_1, \dots, \mathcal{X}_\lambda$ are independent $\text{Pois}(1)$ variables. The rightmost product is defined as 1 when $\mathcal{X}_l = 0$.

Important properties of the estimator are listed in Lemma 1 below. The block-Poisson estimator in (3.4) is a product over λ Poisson estimators; this makes it possible to update the subsampled observations only in a subset of the products, thereby generating a correlation between estimates in successive MCMC iterations; see Section 4. The product form also makes it possible to use fixed, non-random, number of λ factors in the estimator, which simplifies the properties of the estimator. Deligiannidis et al. (2018) show that inducing dependence between likelihood estimates over the MCMC iterations makes it possible to use a much more variable likelihood estimator; this means that much smaller subsamples can be used so that each MCMC iteration is much faster. The reason for using the product of Poisson estimators is to induce correlation, not to reduce the variance of the estimator; see Section 4.2. In fact, Part (v) of Lemma 1 below shows that the variance of the block-Poisson

estimator is the same as the standard Poisson estimator (Papaspiliopoulos, 2009)

$$(3.5) \quad \widehat{L}_P(\theta) := \exp(q(\theta)) \exp(a + \lambda) \prod_{h=1}^G \left(\frac{\widehat{d}_m^{(h)} - a}{\lambda} \right), \quad G \sim \text{Pois}(\lambda),$$

where the product is 1 if $G = 0$. Lemma 1 states some useful properties of the $\widehat{L}_B(\theta)$ estimator.

Lemma 1. *Assume $\sigma_d^2 < \infty$. Then, for any $\theta \in \Theta$,*

- (i) $E[\widehat{L}_B] = L$.
- (ii) *If $\widehat{d}_m^{(h,l)} \geq a$ almost surely for all h and l , then \widehat{L}_B is almost surely non-negative.*
- (iii) $V[|\widehat{L}_B|] < \infty$
- (iv) *For a fixed λ , $V[\widehat{L}_B]$ is minimized at $a = d - \lambda$.*
- (v) $V[\widehat{L}_B(\theta)] = V[\widehat{L}_P(\theta)]$.

Although \widehat{L}_B is unbiased by Part (i) of Lemma 1, Part (ii) shows that the estimator is only positive with probability 1 if a is a lower bound of all $\widehat{d}_m^{(h,l)}$. Section 3.3 shows that it is prohibitively expensive to choose a in this way. We therefore adopt the approach in Lyne et al. (2015) and carry out the pseudo-marginal MCMC on $|\widehat{L}_B|$. Part (iii) ensures that $|\widehat{L}_B|$ has a finite variance. Part (iv) motivates the simplification of setting $a = d - \lambda$ so that it is only necessary to optimize performance with respect to m and λ . Under this simplifying assumption,

$$(3.6) \quad \widehat{L}_B(\theta) = \exp(q(\theta)) \prod_{l=1}^{\lambda} \xi_l, \quad \text{where } \xi_l = \exp\left(\frac{d}{\lambda}\right) \prod_{h=1}^{\mathcal{X}_l} \left(\frac{\widehat{d}_m^{(h,l)} - d}{\lambda} + 1\right).$$

Section 4 derives the optimal tuning parameters m and λ by studying a performance measure involving the variance of the log of the estimator. Since the MCMC is based on $|\widehat{L}_B|$, it is necessary to evaluate the variance of $\log |\widehat{L}_B|$. Lemma 2 gives an expression for this variance assuming that the batch means $\widehat{d}_m^{(h,l)}$ are Gaussian; when m is moderately large this is motivated by the Central Limit Theorem (CLT). For small m , Lemma S7 gives the corresponding result when the $\widehat{d}_m^{(h,l)}$ follow a finite mixture of normals distribution.

Lemma 2. *If $\widehat{d}_m^{(h,l)} \stackrel{iid}{\sim} \mathcal{N}(d, \frac{\gamma}{m})$ for all h and l , then the variance of $\log |\widehat{L}_B|$ when $a = d - \lambda$ is*

$$\sigma_{\log |\widehat{L}_B|}^2 = \lambda(\nu^2 + \eta^2),$$

where

$$\eta := \log \left(\sqrt{\frac{\gamma}{m\lambda^2}} \right) + \frac{1}{2} (\log 2 + \mathbb{E}_J [\psi^{(0)}(1/2 + J)])$$

and

$$\nu^2 := \frac{1}{4} (\mathbb{E}_J [\psi^{(1)}(1/2 + J)] + \mathbb{V}_J [\psi^{(0)}(1/2 + J)]),$$

with $J \sim \text{Pois} \left(\frac{m\lambda^2}{2\gamma} \right)$ and $\psi^{(q)}$ the polygamma function of order q . Furthermore, $\sigma_{\log |\widehat{L}_B|}^2 < \infty$ for all $m > 0$, $\lambda > 0$ and $\gamma > 0$.

The infinite sums in the expectation and variance with respect to the Poisson random variable J in Lemma 2 are accurately approximated by truncation since $\Pr(J = j)$ decreases very quickly to zero as j increases and the polygamma functions are either bounded or grow much slower than the rate of decrease of $\Pr(J = j)$, see the proof of Lemma 2 in Section S8.

3.2. Control variates. Two different types of control variates $q_k(\theta)$ are used to approximate $\ell_k(\theta)$, both based on a Taylor expansion of the log density $\ell_k(\theta) := \log p(y_k | x_k, \theta)$.

The *parameter expanded* control variate suggested by Bardenet et al. (2017) expands $\ell_k(\theta)$ around some reference value θ^* ; it has computational complexity of $O(1)$ (Bardenet et al., 2017) and therefore the overall Computational Cost (CC) for \widehat{L}_B is $m \sum_{l=1}^{\lambda} \mathcal{X}_l$.

Quiroz et al. (2019) present *data expanded* control variates where the expansion of $\ell_k(\theta)$ with respect to $\eta_k = (y_k, x_k)$ is around a reference value of the data η^* . To make the approximation local, a sparse subset of the data is obtained by clustering the data into \mathcal{K} clusters before the MCMC. For each data point η_k belonging to cluster c , $q_k(\theta)$ is an expansion around the centroid η_c^* ; this control variate has a computational complexity of $O(\mathcal{K})$ (Quiroz et al., 2019) and an overall computational cost for \widehat{L}_B of $m \sum_{l=1}^{\lambda} \mathcal{X}_l + O(\mathcal{K})$. See Quiroz et al. (2019) for the asymptotic properties of these two types of control variates with respect to n .

3.3. Soft lower bound. While the lower bound of all $\widehat{d}_m^{(h,l)}$ ensures that \widehat{L}_B is positive (Lemma 1 part (ii)), it is impractical for two reasons. First, for most models it is necessary to evaluate $d_k = \ell_k - q_k$ for all data points to find a lower bound. Second, the optimal implementation outlined in Section 3.1 requires that $\lambda = d - a$. If the control variates are accurate then d is small relative to a , implying that $\lambda \approx -a$. Hence, a large $-a$ implies a large number of products in the block-Poisson estimator, and a large computational cost.

We therefore advocate using a *soft lower bound*, i.e. one that is not necessarily a lower bound for all outcomes of $\widehat{d}_m^{(h,l)}$ but still gives a $\Pr(\widehat{L}_B \geq 0)$ close to one. The soft lower bound makes it possible to obtain negative likelihood estimates, and Section 4.3 shows that $\Pr(\widehat{L}_B \geq 0)$ is a crucial quantity for the efficiency of our method. Lemma 3 gives an analytically tractable expression for this probability.

Lemma 3.

$$\Pr(\widehat{L}_B \geq 0) = \frac{1}{2} \left(1 + (1 - 2\Psi(a, m, \lambda, \gamma))^\lambda \right),$$

where

$$\Psi(a, m, \lambda, \gamma) := \Pr(\xi_l < 0) = \frac{1}{2} \sum_{j=1}^{\infty} \left(1 - (1 - 2\Pr(A_m < 0))^j \right) \Pr(\mathcal{X}_l = j), \quad \mathcal{X}_l \sim \text{Pois}(1),$$

and $A_m := (\widehat{d}_m - d)/\lambda + 1$.

The probability of a positive estimator \widehat{L}_B can be computed whenever $\Pr(A_m < 0)$ is analytically available. By the CLT, we can expect A_m to be approximately normally distributed when m is sufficiently large as \widehat{d}_m will be normal in this case. When m is small, Section S3 of the supplement describes a general approach where \widehat{d}_m is modelled by a mixture of normals.

4. THE SIGNED BLOCK PMMH ALGORITHM

This section outlines the proposed posterior sampling algorithm for the block-Poisson estimator, and derives guidelines for optimally tuning the algorithm.

4.1. The signed PMMH algorithm. Let $p_\Theta(d\theta)$ and $\pi(d\theta) := p(d\theta|y) \propto L(\theta)p_\Theta(d\theta)$ denote the prior and the posterior measures of θ . Let $\widehat{L}(\theta, U)$ be an unbiased, but not

necessarily positive estimator of the likelihood, for example the block-Poisson in (3.4); U is the set of all random variables involved when constructing \widehat{L} and we usually take U to be a set of uniform random numbers with $p_U(du)$ the probability measure of U . The unbiasedness of $\widehat{L}(\theta, U)$ means that

$$(4.1) \quad L(\theta) = \int \widehat{L}(\theta, u) p_U(du), \text{ for any } \theta.$$

It is invalid to define a target posterior measure using the estimator $\widehat{L}(\theta, u)$ because it can be negative. Instead, we define the joint target measure

$$(4.2) \quad \bar{\pi}(d\theta, du) := \frac{1}{\bar{C}} |\widehat{L}(\theta, u)| p_{\Theta}(d\theta) p_U(du), \quad \bar{C} := \int_{\Theta} C(\theta) p_{\Theta}(d\theta), \quad C(\theta) := \int |\widehat{L}(\theta, u)| p_U(du).$$

This is a proper Lebesgue product measure on $\Theta \otimes \mathcal{U}$, and admits the posterior $\pi(d\theta)$ as its marginal measure only if $\widehat{L}(\theta, u) \geq 0$ almost surely. Define

$$(4.3) \quad \bar{\pi}(d\theta) := \int \bar{\pi}(d\theta, du) = \frac{C(\theta) p_{\Theta}(d\theta)}{\bar{C}}.$$

Let $S(\theta, u) := \text{sign}(\widehat{L}(\theta, u)) \in \mathcal{S} := \{-1, 1\}$. An important goal in Bayesian inference is to estimate an integral of the form

$$\mathbb{E}_{\pi}[\psi] = \int_{\Theta} \psi(\theta) \pi(d\theta)$$

for some function $\psi(\theta)$ on Θ . Lyne et al. (2015) cleverly note that

$$(4.4) \quad \mathbb{E}_{\pi}[\psi] = \frac{\int_{\Theta} \psi(\theta) L(\theta) p_{\Theta}(d\theta)}{\int_{\Theta} L(\theta) p_{\Theta}(d\theta)} = \frac{\int_{\Theta} \int_{\mathcal{U}} \psi(\theta) S(\theta, u) \bar{\pi}(d\theta, du)}{\int_{\Theta} \int_{\mathcal{U}} S(\theta, u) \bar{\pi}(d\theta, du)} = \frac{\mathbb{E}_{\bar{\pi}}[\psi S]}{\mathbb{E}_{\bar{\pi}}[S]}.$$

Hence, we can use a pseudo-marginal scheme (Andrieu and Roberts, 2009) to obtain N samples $\{\theta^{(i)}, u^{(i)}, i = 1, \dots, N\}$ from $\bar{\pi}(d\theta, du)$ in (4.2) and then estimate (4.4) by

$$(4.5) \quad \widehat{\mathbb{E}}_{\pi}[\psi] = \frac{\sum_{i=1}^N \psi(\theta^{(i)}) s^{(i)}}{\sum_{i=1}^N s^{(i)}}.$$

Hence, to compute $\mathbb{E}_{\pi}[\psi]$ it is only necessary to store the $\theta^{(i)}$ and the signs $s^{(i)} = S(\theta^{(i)}, u^{(i)})$ in the MCMC.

This elegant observation allows exact inference in the sense that this estimator is guaranteed to converge $\bar{\pi}$ -almost surely to the true value $E_{\pi}[\psi]$ as $N \rightarrow \infty$, even though the θ iterates are distributed as $\bar{\pi}(d\theta) \neq \pi(d\theta)$.

4.2. The signed block PMMH algorithm. Deligiannidis et al. (2018) propose correlating $\log \widehat{L}(\theta, u)$ at the current and proposed MCMC draws using an autoregressive proposal of the underlying random numbers u . This correlated pseudo-marginal algorithm is a substantial advance over the standard PMMH because a much larger $\sigma_{\log \widehat{L}}^2$ can be tolerated without adversely affecting the sampling efficiency.

We now propose an alternative way to correlate the estimates by partitioning U into G blocks and updating only a single random block together with θ in each iteration, keeping the other blocks fixed. In the block-Poisson estimator, we use U_l as the set of random numbers to compute ξ_l , $l = 1, \dots, \lambda$, and group them as

$$(4.6) \quad U = (U_1, \dots, U_G) := U_{1:G},$$

so that each U_i , $i = 1, \dots, G$, contains λ/G of the U_l . Note that we do not require that $G = \lambda$, so the blocks in the block-Poisson estimator do not need to correspond to the blocking of U in (4.6). Section S1.1 shows that $\text{Corr}(\ell(\theta', u'), \ell(\theta, u)) \approx 1 - 1/G$, where (θ, u) and (θ', u') are the current and proposed draws, respectively. This shows that the block-Poisson estimator in (3.4) can produce a pre-specified correlation between the log of the likelihood estimates at successive iterations. Moreover, generating correlation through blocking in a subsampling context is computationally more efficient than using the method in Deligiannidis et al. (2018) since it is unnecessary to work with the whole dataset and to generate the full set of underlying random numbers in each MCMC iteration.

Algorithm 1 outlines the signed block PMMH with the block-Poisson estimator. The MCMC part of the algorithm targets the absolute measure

$$(4.7) \quad \bar{\pi}(d\theta, du_{1:G}) := \frac{p_{\Theta}(d\theta)}{\bar{C}} \prod_{i=1}^G |\widehat{L}^{(i)}(\theta, u_i)| p_{U_i}(du_i),$$

where each $\widehat{L}^{(i)}$ with $E[\widehat{L}^{(i)}] = L(\theta)^{1/G}$ corresponds to the likelihood estimate when using U_i , so that $E\left[\prod_{i=1}^G \widehat{L}^{(i)}\right] = L(\theta)$. Section S1.2 proves the convergence of the MCMC on $\bar{\pi}$ as well as a central limit theorem for the estimator $\widehat{E}_\pi[\psi]$.

Algorithm 1: The signed block PMMH algorithm

Input: Number of blocks G , number of MH iterations N , and initial values $\theta^{(0)}$, $u^{(0)} = (u_1^{(0)}, \dots, u_G^{(0)})$.

Obtain the optimal tuning parameters $\lambda_{\text{opt}}, m_{\text{opt}}$ and a_{opt} from Algorithm 2.

for $i = 1, \dots, N$ **do**

Propose $u' \sim q_U(u^{(i-1)}; du')$ by updating a randomly chosen block $u_g^{(i-1)}$ in $u^{(i-1)}$.

Propose $\theta' \sim q_\Theta(\theta^{(i-1)}; d\theta')$.

Compute $\widehat{L}(\theta', u')$ by Equation (3.4).

Set $(\theta^{(i)}, u^{(i)}) \leftarrow (\theta', u')$ with probability

$$\alpha_{\Theta, U}(\theta^{(i-1)}, u^{(i-1)}, \theta', u') = 1 \wedge \frac{|\widehat{L}(\theta', u')| p_\Theta(\theta')}{|\widehat{L}(\theta^{(i-1)}, u^{(i-1)})| p_\Theta(\theta^{(i-1)})} \frac{q_\Theta(\theta'; d\theta^{(i-1)})}{q_\Theta(\theta^{(i-1)}; d\theta')}$$

else $(\theta^{(i)}, u^{(i)}) \leftarrow (\theta^{(i-1)}, u^{(i-1)})$.

Set $s^{(i)} = S(\theta^{(i)}, u^{(i)})$.

end

Output: Return the estimate

$$\widehat{E}_\pi[\psi] = \frac{\sum_{i=1}^N \psi(\theta^{(i)}) s^{(i)}}{\sum_{i=1}^N s^{(i)}}.$$

4.3. Tuning the signed block PMMH algorithm. This section outlines how to choose the tuning parameters m , λ and a for the signed block PMMH using the block-Poisson estimator. For brevity and clarity, all assumptions, technical details and derivations are in Section S2; we focus here on the main ideas and algorithms. The methodological framework is based on Pitt et al. (2012), which we extend to the signed block PMMH algorithm. Similarly to Pitt et al. (2012), the derived guidelines are based on stylized assumptions that make the analysis tractable and transparent. Section S5 verifies that the guidelines are accurate and robust to deviations from the assumptions. Section S6 presents results for the optimal tuning of the block PMMH when the likelihood estimator is always non-negative.

First, the soft lower bound a is set to its optimal value $a = d - \lambda$, with d replaced by an estimate (see Algorithm 2 below), using the simplified estimator in (3.6). We have found that the randomness from replacing d with an estimate does not affect the tuning procedure.

We now define the objective function which is used to find the optimal λ and m . A natural objective is the computational time needed to obtain the same precision in the importance sampling estimator as that from a single independent Monte Carlo draw from $\pi(\theta)$. Following Pitt et al. (2012), we define the Computational Time (CT) as

$$\text{CT} := \text{Computing cost per iteration} \cdot \frac{V_\pi \widehat{\mathbf{E}}_\pi[\psi]}{V_\pi \widehat{\mathbf{E}}_{\text{MC}}[\psi]},$$

where $V_\pi \widehat{\mathbf{E}}_{\text{MC}}[\psi] = V_\pi(\psi)/N$ is the variance of the ideal Monte Carlo estimator from iid sampling from $\pi(\theta)$, and

$$V_\pi \widehat{\mathbf{E}}_\pi(\psi) = \frac{V_{\bar{\pi}}(\psi S)}{N} \cdot \frac{\text{IF}_{\bar{\pi}, \psi S}}{(2\tau - 1)^2}$$

is the asymptotic variance of the estimator in Algorithm 1 given in Theorem S1 in Section S1.2. $\text{IF}_{\bar{\pi}, \psi S}$ is the usual MCMC inefficiency for samples of ψS from the MCMC targeting the absolute measure $\bar{\pi}(d\theta, du_{1:G})$ in (4.7). The factor $(2\tau - 1)^{-2}$, where $\tau := \Pr(\widehat{L}_B > 0)$, comes from the importance sampling correction for the sign. This gives

$$(4.8) \quad \text{CT} = m\lambda \cdot \frac{V_{\bar{\pi}}(\psi S)}{V_\pi(\psi)} \cdot \frac{\text{IF}_{\bar{\pi}, \psi S}}{(2\tau - 1)^2},$$

where $m\lambda$ is proportional to the expected cost per iteration (the cost is random when using the block-Poisson estimator).

The definition of CT in (4.8) involves $V_{\bar{\pi}}(\psi S)$ which, unlike $\text{IF}_{\bar{\pi}, \psi S}$ (see Section S2), depends on the specific functional ψ . To make the tuning independent on the choice of ψ we derive tuning guidelines under the assumption $V_{\bar{\pi}}(\psi S) = V_\pi(\psi)$. This approximation is expected to be accurate since negative signs are detrimental for the CT, so the optimal m and λ are expected to be in a region where $S = 1$ with probability close to one; see Figure 1 and the discussion below.

Hence, λ and m in Algorithm 1 are chosen by minimizing

$$(4.9) \quad \text{CT}_B(\lambda, m|\gamma) := m\lambda \frac{\text{IF}_{\bar{\pi}, \psi_S} \left(\sigma_{\log|\widehat{L}_B|}^2(\lambda, m|\gamma) \right)}{(2\tau(\lambda, m|\gamma) - 1)^2}.$$

The CT in (4.9) is expressed to show explicitly how each factor depends on the tuning parameters m and λ ; the dependence on γ is also shown. Note in particular that $\text{IF}_{\bar{\pi}, \psi_S}$ is a function of these arguments only through the variance of the log of the absolute value of the block-Poisson estimator. This is analogous to Pitt et al. (2012), except that since the MCMC here is run on $|\widehat{L}_B|$, it is the variance of $\log|\widehat{L}_B|$ that enters the IF; see Section S2 for precise definitions of all the terms in (4.9).

To obtain the CT in (4.9) it is necessary to compute: i) $\sigma_{\log|\widehat{L}_B|}^2$, ii) τ , iii) $\text{IF}(\cdot)$, and iv) $\gamma := n^2\sigma_{d_{u_i}}^2$. The $\text{IF}(\cdot)$ in iii) can be computed by one-dimensional numerical integration; see Lemma S5 in Section S2. The variance $\sigma_{d_{u_i}}^2$ in iv) is the intrinsic variability in the population of differences d_i and can be approximated as in Algorithm 2. Finally, if \widehat{d}_m is assumed normal, then $\sigma_{\log|\widehat{L}_B|}^2$ and τ can be easily computed from Lemmas 2 and 3, respectively. Our recommended strategy is to set $m = 30$, where a CLT motivates the normality of \widehat{d}_m , and optimize CT only with respect to λ . This setting gives the empirical relation $\lambda_{\text{opt}} = \exp(-0.1022 + 0.4904 \log(\gamma_{\text{max}}))$ in Algorithm 2 when $G = 100$ blocks is used ($\rho = 0.99$).

Algorithm 2 summarizes our recommended tuning strategy. The initial optimization in Algorithm 2 is not included in the computational cost since the same optimization initializes all the algorithms in the comparisons. The additional tuning cost in Algorithm 2 is included in our algorithm whenever we compare it against another algorithm. Note that the optimal λ is based on γ_{max} , resulting in a conservatively low variance of the estimator; this is well known to be a good strategy in pseudo-marginal MCMC (Pitt et al., 2012).

Figure 1 plots the CT, $\Pr(\widehat{L} \geq 0)$ and $\sigma_{\log|\widehat{L}_B|}^2$ as functions of λ for this strategy; the figure also shows the optimal value λ_{opt} . Clearly, the optimal λ_{opt} results in a high probability of a positive estimator, regardless of γ .

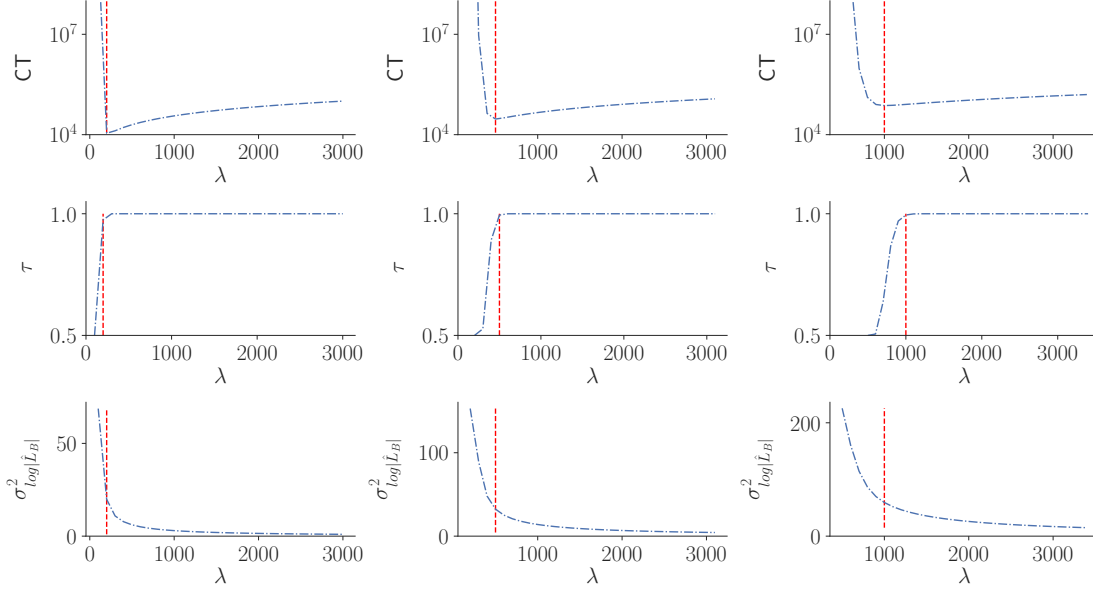


FIGURE 1. Dependence of CT and its parts on λ for the settings in Algorithm 2. The columns correspond to three different γ (left $\gamma = 90,000$, middle $\gamma = 400,000$, right $\gamma = 1,500,000$). The top row shows the Computational Time (CT) in (4.9). The middle row shows the probability of a positive estimator τ in Lemma 3. The bottom rows shows the variance of the log of the absolute value of block-Poisson estimator in (2). The vertical red line marks the optimal value of λ , i.e. λ_{opt} .

Algorithm 2: Tuning strategy for block PMMH with $m = 30$ and $\rho = 0.99$

Input: Number of tuning draws M .

Approximate the posterior by a multivariate student t by optimizing a posterior estimated from a single subsample \tilde{u} of \tilde{m} observations.

for $j = 1, \dots, M$ **do**

- Draw $\theta^{(j)}$ from the approximate Student t posterior
- Estimate $\gamma(\theta^{(j)})$ by $\hat{\gamma}(\theta^{(j)}) = n^2 \hat{\sigma}_{d_{u_i}}^2(\theta^{(j)})$ from the subsample \tilde{u}
- Compute the batch mean $\hat{d}_{\tilde{m}}(\theta^{(j)})$

end

$$\gamma_{\max} = \max\{\hat{\gamma}(\theta^{(1)}), \dots, \hat{\gamma}(\theta^{(M)})\}.$$

$$\bar{d} = M^{-1} \sum_{j=1}^M \hat{d}_{\tilde{m}}(\theta^{(j)}).$$

$$\text{Set } \lambda_{\text{opt}} = \exp(-0.1022 + 0.4904 \log(\gamma_{\max}))$$

$$\text{Set } a_{\text{opt}} = \bar{d} - \lambda_{\text{opt}}.$$

Output: λ_{opt} and a_{opt} .

The reason for setting $m = 30$ in Algorithm 2 is to obtain an easily implemented tuning strategy that ensures that \widehat{d}_m is approximately normal (CLT). However, when \widehat{d}_m is already normal for smaller m , it is beneficial to use a smaller m . In fact, we conjecture that if \widehat{d}_m is normal for any m , the true minimum of (4.9) is obtained with $m_{\text{opt}} = 1$; see Section S4 for some evidence. This is intuitively understood by noting that the computational cost in the CT is proportional to the product $m\lambda$, so the individual m and λ do not matter for the cost. But λ has a much larger effect on increasing τ than m , which explains why it is desirable to spend computational resources on more batches (larger λ) rather than increasing the batch sizes (larger m). Fortunately, Section S4 shows that using $m = 30$ rather than the optimal $m = 1$ only increases CT by a factor of around two, unless $\gamma := n^2\sigma_{d_{u_i}}^2$ is very small, which is unlikely because n is typically very large when subsampling is used. Nevertheless, Section S3 proposes a general tuning strategy where the distribution of \widehat{d}_m is approximated by a mixture of normals. All parts of the CT expression are then available in closed form and the CT can be minimized with respect to both m and λ .

Finally, Section S4 documents that the CT of the signed PMMH with the block-Poisson estimator is 2-3 times larger than for the approximate Subsampling MCMC approach in Quiroz et al. (2019) for most γ , and has up to 8 times larger CT when γ is very small. Hence, there is a trade-off between exactness and computational time.

5. APPLICATIONS

5.1. Model and data. Our experiments consider the logistic regression for $y_i \in \{0, 1\}$ on covariates $x_i \in \mathbb{R}^p$, with distribution

$$p(y_i|x_i, \theta) = \frac{\exp(y_i x_i^\top \theta)}{1 + \exp(x_i^\top \theta)},$$

where θ follows a multivariate normal prior with zero mean and covariance matrix $10I$. We fit the model to the three datasets used in Quiroz et al. (2019): i) the *CovType* data as used in Collobert et al. (2002), with $n = 550,087$ observations and $p = 11$ variables, ii) the firm *Bankruptcy* data as used in Giordani et al. (2014), containing $n = 4,748,089$ observations

and eight covariates, and iii) the *HIGGS* dataset (Baldi et al., 2014) with $n = 1,100,000$ observations and 21 covariates as in Quiroz et al. (2019).

Section S7 contains some additional empirical results from the experiments.

5.2. Experiment 1: Comparisons against Firefly Monte Carlo and MCMC. The first experiment compares the block-Poisson estimator to both Firefly Monte Carlo (Maclaurin and Adams, 2014) and standard MH on the full dataset. Firefly is tuned as in Maclaurin and Adams (2014) with the optimally tuned lower bound for logistic regression based on a central parameter value θ^* and allowing 10% of the observations to change indicator in each iteration. For the block-Poisson estimator we use the parameter expanded control variates, expanded around the same θ^* , resulting in a small $\gamma(\theta)$. The second experiment explores the effect of larger $\gamma(\theta)$. We check that the normality assumption for \hat{d}_m when $m = 30$ is reasonable and Algorithm 2 returns $\lambda_{\text{opt}} = 100$ after rounding to the nearest allowable λ . We simulate $N = 55,000$ samples from the posterior and discard 5,000 as burn-in. A random walk Metropolis proposal is used, with a scaling factor for the posterior covariance at the mode of $2.38/\sqrt{p}$ for MCMC (Roberts et al., 1997) and $2.5/\sqrt{p}$ for subsampling MCMC (Sherlock et al., 2015). We use the same proposal for Firefly Monte Carlo as for MCMC; Maclaurin and Adams (2014) use a similar scaling by targeting the acceptance probability 0.234 (Roberts et al., 1997), but presumably using the identity matrix instead of the posterior covariance at the mode (since both MCMC and their algorithm have very low effective sample sizes in their Table 1). All algorithms are started at θ^* .

We measure the performance of our subsampling MCMC using an empirical version of the CT in (4.9); the IF for the chain $\{s_i\theta_i, i = 1, 2, \dots, N\}$ is estimated using the `coda` package in R (Plummer et al., 2006); the cost is taken as the average number of evaluations over the MCMC iterations used when forming the estimator (the number of terms within a factor in the product is random); and τ is replaced by its empirical estimate. For MCMC we use a similar measure but set $\tau = 1$ and the number of evaluations to n . We define the estimated Relative Computational Time (RCT) for the block-Poisson algorithm \mathcal{B} against

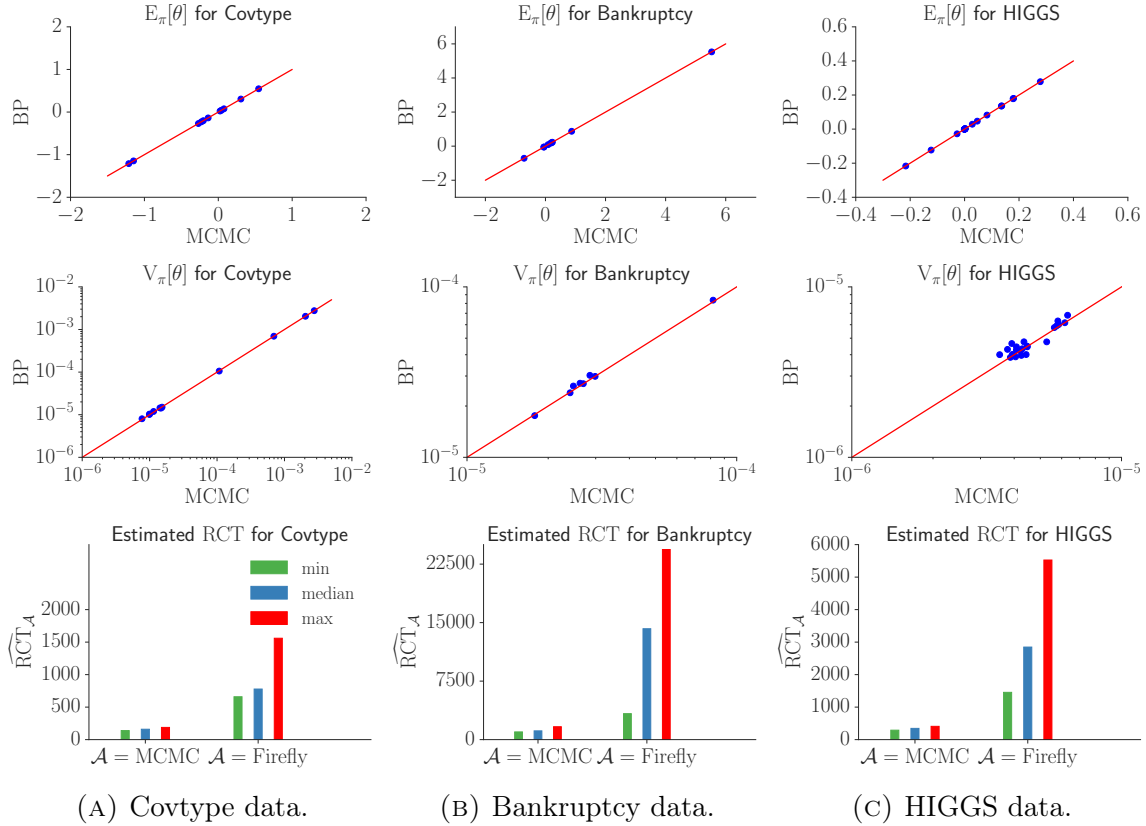


FIGURE 2. Results from Experiment 1 using parameter expanded control variates. Estimates of posterior expectation (upper), variance (middle) and Relative Computational Time (RCT) in (5.1) (lower) of correlated product-Poisson with $\lambda = 100$ relative to MCMC and Firefly Monte Carlo. The results are shown for three datasets, Covtype (A), Bankruptcy (B) and HIGGS (C).

any algorithm \mathcal{A} with $\tau = 1$ as

$$(5.1) \quad \widehat{\text{RCT}}_{\mathcal{A}} := \frac{\overline{\text{CC}}_{\mathcal{A}} \times \widehat{\text{IF}}_{\mathcal{A}}}{\overline{\text{CC}}_{\mathcal{B}} \times \widehat{\text{IF}}_{\mathcal{B}} / (2\widehat{\tau}_{\mathcal{B}} - 1)^2},$$

where CC is the computational cost introduced in Section 3.2 and the bars denote averages over MCMC iterations. This RCT measures how much computational resources that algorithm \mathcal{A} , compared to the block-Poisson algorithm \mathcal{B} , consumes in order to produce a posterior estimate with a given precision; see, e.g., Appendix C of Tran et al. (2017) and Quiroz et al. (2019) for more details.

Figure 2 shows the accuracy of estimating the posterior expectations and variances using our method on the three datasets. Although some estimates are visually off the 45-degree

line, all deviations are within the usual Monte Carlo error, and we conclude that the estimates are very accurate. Figure 2 also shows the relative computational times in (5.1) compared to MCMC and Firefly Monte Carlo, respectively; the block-Poisson approach has a two orders of magnitude improvement against MCMC and three or even four orders of magnitude against Firefly Monte Carlo. Although Firefly Monte Carlo has a lower computational cost than MCMC (less density evaluations), its extreme autocorrelation (documented in Section S7) grossly inflates the CT.

5.3. Experiment 2: Performance when the control variates are poor. The next experiment is a serious test of the methodology when the control variates are poor so that γ is large and there are outliers in the differences d_k . To obtain poor covariates, we use the data expanded control variates in Quiroz et al. (2019), with a very small number of clusters in relation to n . We follow Quiroz et al. (2019) and choose $K = 1042, 16374, 355$ for the Covtype, Bankruptcy and HIGGS datasets. The deliberately poor control variates generate severe outliers in the d_k population and normality is therefore not guaranteed for $m = 30$. We found that $m = 100, 100, 600$ are large enough to obtain normality in the Covtype, Bankruptcy and HIGGS datasets, respectively, and the corresponding optimal λ are $\lambda_{\text{opt}} = 500, 1100, 300$. The other settings are the same as in Experiment 1.

Figure 3 summarizes the results. Although the control variates are now significantly less accurate than in Experiment 1, our algorithm is still more efficient than MCMC and dramatically more efficient than Firefly Monte Carlo. Note that Firefly Monte Carlo is based on the same tight lower bound as in Experiment 1, yet our algorithm with poor control variates still performs much better. This example illustrates that even when γ is large and varies a lot over the parameter space, our guidelines suggest a λ which results in an efficient MCMC chain that still outperforms MH on the full dataset and Firefly Monte Carlo.

5.4. Experiment 3: Comparisons against zig-zag — scaling with respect to p . The third experiment explores how the performance of MCMC with the block-Poisson estimator scales with the number of parameters, p , and how it compares with the recently proposed zig-zag sampler with subsampling.

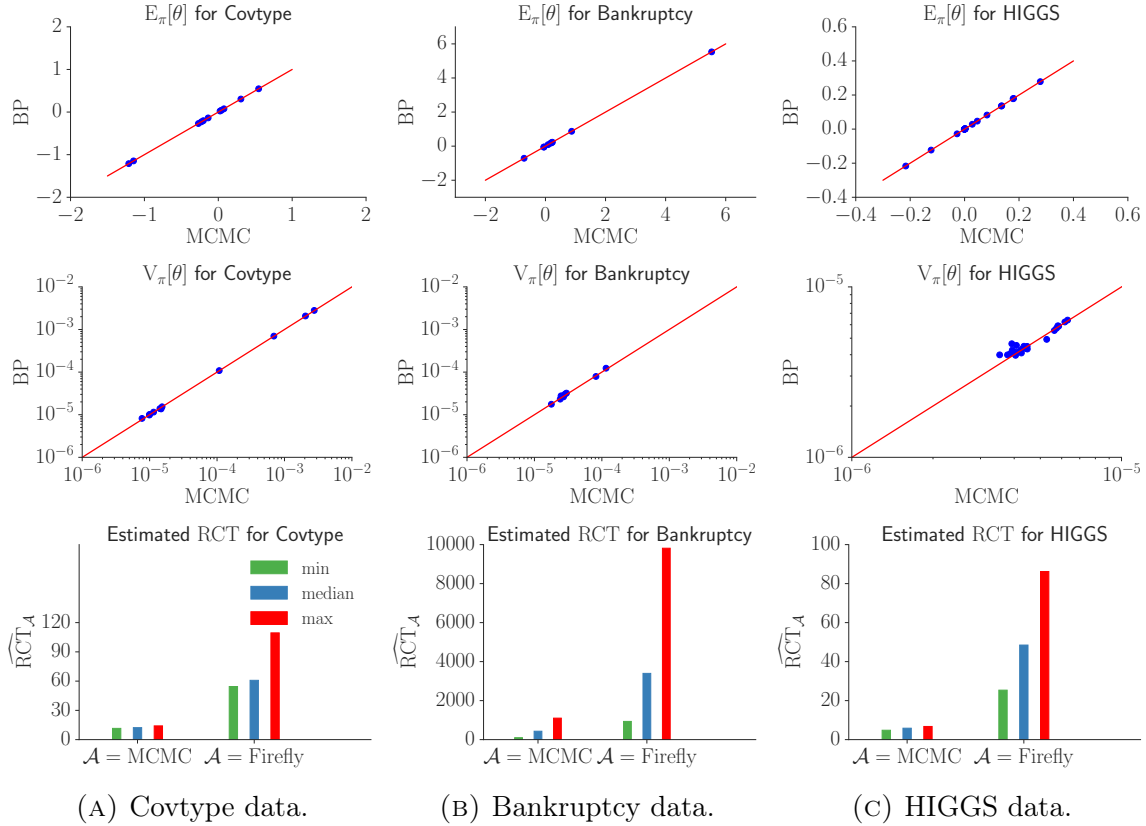


FIGURE 3. Results from Experiment 2 using data expanded control variates with large γ . Estimates of posterior expectation (upper), variance (middle) and Relative Computational Time (RCT) in (5.1) (lower) of block-Poisson with $\lambda = 500, 1100, 300$ (Covtype, Bankruptcy, HIGGS) relative to MCMC and Firefly Monte Carlo. The results are shown for three datasets, Covtype (A), Bankruptcy (B) and HIGGS (C).

The zig-zag process in Bierkens et al. (2019) is a *continuous time* piecewise deterministic multivariate Markov process set up so that it has the posterior of interest as its invariant distribution. The process evolves deterministically in time in a linear fashion until one of its components changes direction (sign). The time to this event, i.e. the switching time, is a random variable that is controlled by *switching rates*, one for each component. A rejection sampling step determines if the component with lowest switching rate makes a switch. This rejection step requires upper bounds of the switching rates for each dimension; the looser the bound, the lower is the acceptance probability. Importantly, the analytical bounds need to be derived for every new model, making it hard to automate the zig-zag sampler, whereas

in our algorithm the gradient and Hessian of the log density needed for the control variates are readily computed using automatic differentiation.

Bierkens et al. (2019) also propose a subsampling variant of this algorithm where, in each zig-zag iteration, *a single data point* is required to determine the probability of a switch. When used with control variates, the performance of zig-zag with subsampling is shown by Bierkens et al. (2019) to be super-efficient and they demonstrate impressive performance for logistic regression with a small number of parameters.

We now compare our method with the zig-zag subsampling algorithm in a logistic regression setup, using their code at <https://github.com/jbierkens/zigzag-experiments>. To make the comparison with zig-zag fair, we implement our exact subsampling algorithm using a proposal for θ based on Hamiltonian dynamics (Neal, 2011), following Dang et al. (2019) who propose an efficient way to use data subsampling in Hamiltonian Monte Carlo (HMC). A Hamiltonian proposal uses a continuous time dynamics to explore the posterior more efficiently and this time-continuity makes it more similar to the zig-zag sampler; see Nishimura et al. (2017) for a connection between their discontinuous Hamiltonian Monte Carlo (HMC) algorithm and the zig-zag sampler. This proposal also has the added benefit of demonstrating that our subsampling approach applies to HMC samplers. We follow Dang et al. (2019) and set the stepsize $\epsilon = 0.2$ for the discretization of the Hamiltonian dynamics and use $L = 6$ leap-frog steps for solving the dynamics. The Poisson estimator is implemented with $m = 30$ and $\lambda = 100$, using 3,000 subsamples used on average.

We follow Bierkens et al. (2019) and use epochs as the computational budget. One epoch corresponds to the number of iterations required to evaluate the gradient of all n data points. Since zig-zag evaluates the gradient of the full dataset in each iteration, one epoch is 1 iteration. For zig-zag with subsampling one epoch is n iterations since it evaluates the gradient of a single data point in each iteration. Our HMC based method uses L evaluations of the gradient of the log-density and a log-density evaluation for each of the $m\lambda$ subsamples for updating θ given u . Since we only change one block of u in the update step for $u|\theta$, this step uses m log-density evaluations; see Dang et al. (2019) for details. Thus the number of

iterations per epoch for our method is therefore

$$\frac{n}{(L+1) \cdot \lambda m + m} = \frac{1,100,000}{(6+1) \cdot 1,000 \cdot 30 + 30} \approx 52,306,$$

for our settings.

We use the HIGGS dataset for this experiment since it has the largest number of covariates among the three datasets, $p = 22$, including an intercept. For each $j = 2, \dots, 22$, we run the algorithms on a dataset consisting of the first $p = j$ covariates (including the intercept) and compare the effective sample sizes obtained. Figure 4 shows, for each p , the median effective sample size of the parameters when using a computational budget of 1,000 epochs for both zig-zag algorithms. The effective sample size is defined as the number of samples N divided by the inefficiency factor. Clearly, the subsampling zig-zag sampler is extremely efficient for small p ; for $p = 2$ it is approximately a factor 56 times more efficient than our algorithm. However, the efficiency of subsampling zig-zag deteriorates when p increases, since the acceptance probability that determines the switch decreases, indicating that the bounds lose their tightness as discussed above. Note that the efficiency of our method remains essentially unchanged with dimension. With $p = 15$, our method is 1.6 times more efficient than zig-zag, and for $p = 22$ our approach is 3.2 times more efficient. The performance of zig-zag depends on the tightness of the upper bound, and it is unclear that equally tight bounds are readily available for more complex models.

6. CONCLUSIONS

We propose an algorithm for fast exact simulation-based inference where the likelihood is estimated cheaply by efficient data subsampling. At the core of the algorithm is a novel and unbiased block-Poisson estimator of the likelihood targeting a given correlation between estimates at successive MCMC iterations, which is known to increase the efficiency (Deligiannidis et al., 2018).

For computational reasons, the block-Poisson estimator is set up to allow for occasional negative likelihood estimates. The proposed algorithm is therefore a signed PMMH algorithm

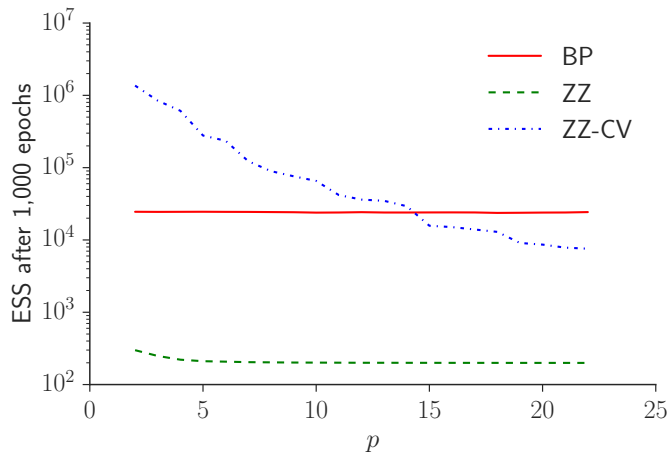


FIGURE 4. Effective sample size (ESS) after 1,000 epochs vs the number of parameters p ; ESS is the median over parameters. The results are shown for the block-Poisson sampler with a Hamiltonian proposal (BP), zig-zag sampler (ZZ), and zig-zag sampler with subsampling and control variates (ZZ-CV). The vertical axis is in logarithmic scale.

(Lyne et al., 2015) where the pseudo-marginal MCMC is based on the absolute value of the likelihood estimate followed by a sign-correcting importance sampling step.

A major contribution of the article is the derivation of practical guidelines for tuning the parameters in the signed PMMH algorithm by minimizing the asymptotic variance of the importance sampling estimator per unit of computing time. The guidelines are based on idealized assumptions, but we demonstrate that the guidelines are accurate, effective and robust to features of the data. The framework proposed here applies to a larger set of problems, in particular models with intractable normalizing constants.

We demonstrate the performance of our algorithm by applying it to three commonly used datasets that are modelled by logistic regression. The proposed algorithm dramatically outperforms MH on the full dataset and Firefly Monte Carlo, and is shown to scale better with respect to the dimension of the parameter space than the zig-zag subsampling algorithm.

7. ACKNOWLEDGMENTS

We thank the Editor, Associate Editor and two reviewers for helping improve both the content and presentation of the article. Matias Quiroz, Robert Kohn and Khue-Dung Dang were partially financially supported by Australian Research Council Center of Excellence grant

CE140100049. Mattias Villani was partially financially supported by Swedish Foundation for Strategic Research (Smart Systems: RIT 15-0097).

REFERENCES

- Andrieu, C. and Roberts, G. O. (2009). The pseudo-marginal approach for efficient Monte Carlo computations. *The Annals of Statistics*, 37(2):697–725.
- Baldi, P., Sadowski, P., and Whiteson, D. (2014). Searching for exotic particles in high-energy physics with deep learning. *Nature Communications*, 5.
- Banterle, M., Grazian, Clara, L. A., and Robert, C. P. (2019). Accelerating Metropolis-Hastings algorithms by delayed acceptance. *Foundations of Data Science*, 1:103.
- Bardenet, R., Doucet, A., and Holmes, C. (2014). Towards scaling up Markov chain Monte Carlo: an adaptive subsampling approach. In *Proceedings of The 31st International Conference on Machine Learning*, pages 405–413.
- Bardenet, R., Doucet, A., and Holmes, C. (2017). On Markov chain Monte Carlo methods for tall data. *Journal of Machine Learning Research*, 18(47):1–43.
- Bierkens, J., Fearnhead, P., and Roberts, G. (2019). The zig-zag process and super-efficient sampling for Bayesian analysis of big data. *The Annals of Statistics*, 47(3):1288–1320.
- Bouchard-Côté, A., Vollmer, S. J., and Doucet, A. (2018). The bouncy particle sampler: A nonreversible rejection-free Markov chain Monte Carlo method. *Journal of the American Statistical Association*, 113(522):855–867.
- Collobert, R., Bengio, S., and Bengio, Y. (2002). A parallel mixture of SVMs for very large scale problems. *Neural Computation*, 14(5):1105–1114.
- Dang, K.-D., Quiroz, M., Kohn, R., Tran, M.-N., and Villani, M. (2019). Hamiltonian Monte Carlo with energy conserving subsampling. *Journal of Machine Learning Research*, 20(100):1–31.
- Deligiannidis, G., Doucet, A., and Pitt, M. K. (2018). The correlated pseudomarginal method. *Journal of the Royal Statistical Society: Series B (Statistical Methodology)*, 80(5):839–870.

- Doucet, A., Pitt, M., Deligiannidis, G., and Kohn, R. (2015). Efficient implementation of Markov chain Monte Carlo when using an unbiased likelihood estimator. *Biometrika*, 102(2):295–313.
- Feller, W. (2008). *An Introduction to Probability Theory and its Applications*, volume 2. John Wiley & Sons.
- Giordani, P., Jacobson, T., Von Schedvin, E., and Villani, M. (2014). Taking the twists into account: Predicting firm bankruptcy risk with splines of financial ratios. *Journal of Financial and Quantitative Analysis*, 49(4):1071–1099.
- Hastings, W. K. (1970). Monte Carlo sampling methods using Markov chains and their applications. *Biometrika*, 57(1):97–109.
- Jacob, P. E. and Thiery, A. H. (2015). On nonnegative unbiased estimators. *The Annals of Statistics*, 43(2):769–784.
- Korattikara, A., Chen, Y., and Welling, M. (2014). Austerity in MCMC land: Cutting the Metropolis-Hastings budget. In *Proceedings of the 31st International Conference on Machine Learning (ICML-14)*, pages 181–189.
- Li, R., Wang, X., Zha, H., and Tao, M. (2020). Improving sampling accuracy of stochastic gradient MCMC Methods via non-uniform subsampling of gradients. *arXiv preprint arXiv:2002.08949*.
- Lyne, A.-M., Girolami, M., Atchade, Y., Strathmann, H., and Simpson, D. (2015). On Russian roulette estimates for Bayesian inference with doubly-intractable likelihoods. *Statistical Science*, 30(4):443–467.
- Maclaurin, D. and Adams, R. P. (2014). Firefly Monte Carlo: Exact MCMC with subsets of data. In *Proceedings of the 30th Conference on Uncertainty in Artificial Intelligence (UAI 2014)*.
- Metropolis, N., Rosenbluth, A. W., Rosenbluth, M. N., Teller, A. H., and Teller, E. (1953). Equation of state calculations by fast computing machines. *The Journal of Chemical Physics*, 21(6):1087–1092.

- Meyn, S. P. and Tweedie, R. L. (2012). *Markov Chains and Stochastic Stability*. Springer Science & Business Media.
- Neal, R. M. (2011). MCMC using Hamiltonian dynamics. *Handbook of Markov Chain Monte Carlo*, 2:113–162.
- Nishimura, A., Dunson, D., and Lu, J. (2017). Discontinuous Hamiltonian Monte Carlo for discrete parameters and discontinuous likelihoods. *arXiv preprint arXiv:1705.08510*.
- Papaspiliopoulos, O. (2009). A methodological framework for Monte Carlo probabilistic inference for diffusion processes. *Manuscript*. Available at http://wrap.warwick.ac.uk/35220/1/WRAP_Papaspiliopoulos_09-31w.pdf.
- Pav, S. E. (2015). Moments of the log non-central chi-square distribution. *arXiv preprint arXiv:1503.06266*.
- Payne, R. D. and Mallick, B. K. (2018). Two-stage Metropolis-Hastings for tall data. *Journal of Classification*, 35:29–51.
- Pitt, M. K., Silva, R. S., Giordani, P., and Kohn, R. (2012). On some properties of Markov chain Monte Carlo simulation methods based on the particle filter. *Journal of Econometrics*, 171(2):134–151.
- Plummer, M., Best, N., Cowles, K., and Vines, K. (2006). CODA: Convergence diagnosis and output analysis for MCMC. *R News*, 6(1):7–11.
- Quiroz, M., Kohn, R., Villani, M., and Tran, M.-N. (2019). Speeding up MCMC by efficient data subsampling. *Journal of the American Statistical Association*, 114(526):831–843.
- Quiroz, M., Tran, M.-N., Villani, M., and Kohn, R. (2018a). Speeding up MCMC by delayed acceptance and data subsampling. *Journal of Computational and Graphical Statistics*, 27(1):12–22.
- Quiroz, M., Villani, M., Kohn, R., Tran, M.-N., and Dang, K.-D. (2018b). Subsampling MCMC - An introduction for the survey statistician. *Sankhya A*, 80(1):33–69.
- Rhee, C. and Glynn, P. W. (2015). Unbiased estimation with square root convergence for SDE models. *Operations Research*, 63(5):1026–1043.

- Roberts, G. O., Gelman, A., and Gilks, W. R. (1997). Weak convergence and optimal scaling of random walk Metropolis algorithms. *The Annals of Applied Probability*, 7(1):110–120.
- Roberts, G. O. and Rosenthal, J. S. (2004). General state space Markov chains and MCMC algorithms. *Probability Surveys*, 1:20–71.
- Salomone, R., Quiroz, M., Kohn, R., Villani, M., and Tran, M.-N. (2020). Spectral subsampling MCMC for stationary time series. *arXiv preprint arXiv:1910.13627v2*.
- Sherlock, C., Thiery, A. H., Roberts, G. O., and Rosenthal, J. S. (2015). On the efficiency of pseudo-marginal random walk Metropolis algorithms. *The Annals of Statistics*, 43(1):238–275.
- Tran, M.-N., Kohn, R., Quiroz, M., and Villani, M. (2017). The block pseudo-marginal sampler. *arXiv preprint arXiv:1603.02485v5*.
- Van der Vaart, A. W. (1998). *Asymptotic Statistics*, volume 3. Cambridge University Press.
- Wagner, W. (1988). Unbiased multi-step estimators for the Monte Carlo evaluation of certain functional integrals. *Journal of Computational Physics*, 79(2):336–352.
- Walck, C. (1996). Hand-book on statistical distributions for experimentalists. Technical report. <http://inspirehep.net/record/1389910/files/suf9601.pdf>.

We refer to equations, sections, lemmas in the main paper as Equation 1, Section 1, Lemma 1 etc., and to equations, sections and lemmas, etc in the supplement as Equation (S1), Section S1 and Lemma S1, etc.

The supplement is organized as follows. Section S1 presents some properties of the signed block PMMH algorithm. Section S2 derives a tractable formula for the inefficiency factor of the algorithm. Section S3 shows a more general approach to obtain the optimal tuning for the signed block PMMH algorithm. Section S4 compares the computational time between the block-Poisson estimator and the approximate method in Quiroz et al. (2019). Section S5 evaluates the robustness of the tuning guideline to deviations from its assumption. Section S6 analyses a special case of the signed block PMMH algorithm when the estimator is almost surely positive. Section S7 provides some additional details for the experiments in Section 5. Section S8 provides the proofs of some results in the paper and the supplement.

S1. PROPERTIES OF THE SIGNED BLOCK PMMH ALGORITHM

S1.1. Correlation from blocking. We first show that the correlation induced by block PMMH has a simple form. Let $u := (u_1, \dots, u_G)$ and $u' := (u'_1, \dots, u'_G)$ denote the current and proposed values of U , respectively. We will write $u_i \in \mathcal{U}$ for $i = 1, \dots, G$, so that $u_{1:G} \in \mathcal{U}^G$. Then

Lemma S1. U_1, \dots, U_G are independent ($\bar{\pi}$) conditional on θ , i.e., $\bar{\pi}(u_{1:G}|\theta) = \prod_{i=1}^G \pi(u_i|\theta)$.

Let $\ell(\theta', u') = \log |\widehat{L}_B(\theta', u')|$ and $\ell(\theta, u) = \log |\widehat{L}_B(\theta, u)|$. Then,

$$\ell(\theta', u') = \sum_{i=1}^G \log |L^{(i)}(\theta', u'_i)| \quad \text{and} \quad \ell(\theta, u) = \sum_{i=1}^G \log |L^{(i)}(\theta, u_i)|;$$

$\ell(\theta', u')$ and $\ell(\theta, u)$ have $G-1$ out of G terms of the u_i in common, and the u_i are independent by Lemma S1. Hence, for G large and θ close to θ' , we argue that $\ell(\theta', u')$ and $\ell(\theta, u)$ are approximately normal with a correlation close to $\rho = 1 - \frac{1}{G}$. Furthermore, if the sample size is large, then θ and θ' are likely to be close by the Bernstein von Mises theorem (Van der Vaart, 1998, Chapter 10.2). In our case $G = 100$ and the sample size n is large. Hence, $\text{Corr}(\ell(\theta', u'), \ell(\theta, u)) \approx 1 - 1/G$, which demonstrates why the block-Poisson estimator in

(3.4) allows us to target a given correlation between the log of the likelihood estimator at the current and proposed draws.

S1.2. Convergence of the signed block PMMH algorithm. The proposal distribution updating a single block at random is

$$(S1.1) \quad q_U(u; du') := \frac{1}{G} \sum_{i=1}^G p_{U_i}(du'_i) \prod_{j \neq i} \delta_{u_j}(du'_j),$$

where $\delta_a(\cdot)$ is the Dirac delta measure centered at a . Let $q_\Theta(\theta; d\theta')$ be the proposal for θ so that the joint proposal for θ and u is $q_\Theta(\theta; d\theta')q_U(u; du')$. Consider now the signed block Metropolis-Hastings sampling scheme for θ and u .

Algorithm S1: Block PMMH sampling for the absolute measure

Input: Current values of θ, u .

Generate θ', u' using the proposal $q_\Theta(\theta; d\theta')q_U(u; du')$.

Set $\theta \leftarrow \theta'$ and $u \leftarrow u'$ with probability

$$\alpha_{\Theta, U}(\theta, u, \theta', u') = 1 \wedge \frac{\bar{\pi}(d\theta', du')}{\bar{\pi}(d\theta, du)} \times \frac{q_\Theta(\theta'; d\theta)q_U(u'; du)}{q_\Theta(\theta; d\theta')q_U(u; du')}.$$

Output: New values of θ, u .

The next lemma gives a workable expression for the acceptance probability of Algorithm S1.

Lemma S2.

$$(S1.2) \quad \frac{\bar{\pi}(d\theta', du')}{\bar{\pi}(d\theta, du)} \times \frac{q_\Theta(\theta'; d\theta)q_U(u'; du)}{q_\Theta(\theta; d\theta')q_U(u; du')} = \frac{|\widehat{L}(\theta', u')|p_\Theta(d\theta')}{|\widehat{L}(\theta, u)|p_\Theta(d\theta)} \frac{q_\Theta(\theta'; d\theta)}{q_\Theta(\theta; d\theta')}.$$

Theorem S1 below proves the ergodic properties of Algorithm S1 based on assumptions about the following sampling scheme targeting the intractable $\bar{\pi}(d\theta)$ and some additional conditions stated in Assumption S1.

Assumption S1.

- (i) For all $\theta \in \Theta$ and $u \in \mathcal{U}^G$, $-\infty < \widehat{L}(\theta, u) < \infty$ and $C(\theta) > 0$, where $C(\theta)$ is defined in (4.2).

Algorithm S2: MH sampling for the θ -marginal absolute measure

Input: Current value of θ .

Generate θ' using the proposal $q_{\Theta}(\theta; d\theta')$.

Set $\theta \leftarrow \theta'$ with probability

$$\alpha_{\Theta}(\theta, \theta') = 1 \wedge \frac{\bar{\pi}(d\theta')q(\theta'; d\theta)}{\bar{\pi}(d\theta)q(\theta; d\theta')}.$$

Output: New value of θ .

- (ii) Let $P_{\Theta}(\theta; d\theta') = K_{\Theta}(\theta; d\theta') + \delta_{\theta}(d\theta') (1 - \int K_{\Theta}(\theta; d\theta'))$ and $K_{\Theta}(\theta; d\theta') = \alpha_{\Theta}(\theta, \theta')q_{\Theta}(\theta; d\theta')$ be the Markov transition kernel and sub-stochastic kernel of Algorithm S2. We assume that if $P_{\Theta}(\theta; B) > 0$ for some θ and B with $\bar{\pi}(B) > 0$, then $K_{\Theta}(\theta; B) > 0$.

If $\theta' \neq \theta$, then $K_{\Theta}(\theta; d\theta) = q_{\Theta}(\theta; d\theta)$ and $P_{\Theta}(\theta; d\theta') = K_{\Theta}(\theta; d\theta')$; a sufficient condition for Assumption S1(ii) is that if $P_{\Theta}(\theta; d\theta) > 0$ then $q_{\Theta}(\theta; d\theta) > 0$; i.e. the proposal kernel $q_{\Theta}(\theta; \cdot) > 0$ whenever the transition probability $P_{\Theta}(\theta; d\theta) > 0$.

Theorem S1 gives some convergence properties of the block PMMH sampling scheme for $\bar{\pi}(\cdot, \cdot)$; Part (iii) and (iv) of Theorem S1 were also obtained by Lyne et al. (2015).

Theorem S1. *Suppose that the Markov chain in Algorithm S2 is irreducible and aperiodic and that Assumption S1 holds. Then,*

- (i) *Algorithm S1 is reversible.*
- (ii) *Samples from Algorithm S1 converges to $\bar{\pi}$ in total variation norm.*
- (iii) *Suppose also that $E_{\pi}[|\psi|] < \infty$ and $E_{\bar{\pi}}(S) \neq 0$. Then, $\widehat{E}_{\pi}[\psi] \rightarrow E_{\pi}[\psi]$ $\bar{\pi}$ -almost surely.*
- (iv) *Define the Inefficiency Factor (IF)*

$$(S1.3) \quad \text{IF}_{\bar{\pi}, \psi S} = \frac{V_{\bar{\pi}}(\psi S) + 2 \sum_{j=1}^{\infty} \Gamma_j}{V_{\bar{\pi}}(\psi S)},$$

where $\Gamma_j = \text{Cov}_{\bar{\pi}}(S_0\psi(\theta_0), S_j\psi(\theta_j))$ and $\{(\theta_0, S_0), \dots, (\theta_j, S_j), \dots\}$ are the MCMC iterates generated by the sampling scheme in Algorithm S1. If $V_{\bar{\pi}}[\psi S] \text{IF}_{\bar{\pi}, \psi S} < \infty$ and $E_{\bar{\pi}}(S) \neq 0$, then

$$(S1.4) \quad \sqrt{N} \left(\widehat{E}_{\pi}(\psi) - E_{\pi}(\psi) \right) \xrightarrow{d} \mathcal{N} \left(0, \frac{V_{\bar{\pi}}(\psi S) \text{IF}_{\bar{\pi}, \psi S}}{E_{\bar{\pi}}(S)^2} \right), \text{ and } E_{\bar{\pi}}(S)^2 = (2\tau - 1)^2.$$

S2. THE INEFFICIENCY FACTOR FOR SIGNED BLOCK PMMH

This section presents the framework for obtaining heuristic guidelines for choosing λ and m in Section 4. In particular, we obtain a tractable expression for the inefficiency factor for the signed block PMMH sampler, which is used for minimizing the computational time CT_B . The analysis follows Pitt et al. (2012), and our simplifying assumptions are in the same spirit.

Define,

$$(S2.1) \quad C_i(\theta) = \int_U |\widehat{L}^{(i)}(\theta, u_i)| p_U(du_i), \quad \widetilde{Z}_i(\theta, u_i) = \log |\widehat{L}^{(i)}(\theta, u_i)| - \log C_i(\theta), \quad i = 1, \dots, G,$$

$$Z(\theta, u) = \sum_{i=1}^G \widetilde{Z}_i(\theta, u_i) \quad \text{and} \quad \widetilde{Z}_{1:G} = (\widetilde{Z}_1, \dots, \widetilde{Z}_G).$$

Lemma S3 justifies the mapping of (θ, u) into a more tractable set of variables. Its proof is straightforward and omitted.

Lemma S3.

$$(S2.2) \quad \begin{aligned} \bar{\pi}(d\theta, du) &= \exp(z) \bar{\pi}(d\theta) \prod_{i=1}^G p_{U_i}(du_i), & \bar{\pi}(d\widetilde{z}_{1:G}|\theta) &= \prod_{i=1}^G \exp(\widetilde{z}_i) p_{Z_i}(d\widetilde{z}_i), \\ \mathbb{E}_{u_i \sim p_{U_i}} \left(\exp(\widetilde{Z}_i) \mid \theta \right) &= 1 & \text{and} & \quad \mathbb{E}_{u \sim p_U} \left(\exp(Z) \mid \theta \right) = 1, \end{aligned}$$

with $\bar{\pi}(d\theta)$ in (4.3).

Equation (S2.2) shows that the \widetilde{z}_i are $\bar{\pi}$ -independent conditional on θ . Let $v = \widehat{L}(\theta, u)$ and take w such that (θ, v, z, w) is a diffeomorphism of (θ, u) . Then, $p(d\theta, dv, dz, dw) = p(d\theta, du)$. This allows the transformation of the measure $\bar{\pi}(\theta, u)$ to a workable expression in Lemma S4. Next, we assume that,

Assumption S2. $S := \text{sign}(\widehat{L}(\theta, U))$ and $Z(\theta, U)$ are $\bar{\pi}$ -independent given θ .

Assumption S2 is reasonable as Z is defined in terms of the absolute value of the estimator and therefore ignores the sign.

Lemma S4. *Suppose that Assumption S2 holds. Then,*

$$(S2.3) \quad \bar{\pi}(d\theta, ds, dz) = \exp(z)\bar{\pi}(d\theta)p(ds|\theta)p(dz|\theta).$$

Similarly to Pitt et al. (2012), we consider a hypothetical chain targeting (S2.3). The following assumption presents the idealized proposal which makes the derivation of the inefficiency tractable.

Assumption S3.

(i) *If $U_i \sim p_{U_i}(\cdot), i = 1, \dots, G$, then the distribution of $Z = \sum_{i=1}^G \tilde{Z}_i(\theta, U_i)$ conditional on θ is $\mathcal{N}(-\sigma^2/2, \sigma^2)$ with $\sigma^2 := \text{V}_{u \sim p_U}[Z]$, which is independent of θ .*

(ii) *$q(\theta, s, z; d\theta', ds', dz') = \bar{\pi}(d\theta')p(ds'|\theta')q(z; dz'|\sigma^2, \rho)$, with $\rho = 1 - \frac{1}{G}$ and*

$$(S2.4) \quad q(z; dz'|\rho, \sigma^2) = \mathcal{N}\left(dz' \left| -\frac{\sigma^2}{2}(1 - \rho) + \rho z, \sigma^2(1 - \rho^2) \right.\right) \text{ for } \rho = 1 - \frac{1}{G}.$$

The mean of z in Part (i) of Assumption S3 is $-1/2$ of the variance, which is now consistent with the fact that $\text{E}_{u \sim p_U}[e^Z] = 1$. This implies that, if $Z \sim \bar{\pi}$, then $Z \sim \mathcal{N}(\sigma^2/2, \sigma^2)$. The proposal $q(z; dz'|\rho, \sigma^2)$ in Part (ii) of Assumption S3 implies that the correlation between the current z and proposal z' is $\rho = 1 - 1/G$. The assumption that $\rho = 1 - 1/G$ is plausible because the current Z and proposed Z' differ only by one block; see also the discussion at the end of Section 4.2. The inefficiency factor for the independent pseudo-marginal method in Pitt et al. (2012) is derived using $\rho = 0$. The next lemma uses their proof, but with the proposal in (S2.4).

Lemma S5. *Suppose that Assumption S3 holds. Then,*

(i) *The MH acceptance probability of the proposal $q(\theta, s, z; d\theta', ds', dz')$ is*

$$\min\{1, \exp(z' - z)\}.$$

(ii) *The acceptance probability conditional on z of the idealized sampling scheme is*

$$k(z|\sigma^2, \rho) = \int \min\{1, \exp(z' - z)\}q(z; dz'|\sigma^2, \rho).$$

(iii) *The inefficiency of the sampling scheme is*

$$\text{IF}_{\bar{\pi}}(\sigma^2, \rho) = 1 + 2\mathbb{E}_{\bar{\pi}(z|\theta)}\left(\frac{1 - k(z|\sigma^2, \rho)}{k(z|\sigma^2, \rho)}\right),$$

where

$$(S2.5) \quad k(z|\sigma^2, \rho) = \exp(-x + w^2/2)\Phi\left(\frac{x}{w} - w\right) + \Phi\left(\frac{-x}{w}\right),$$

with $x := \left(z + \frac{\sigma^2}{2}\right)(1 - \rho)$, $w := \sigma\sqrt{1 - \rho^2}$ and Φ denotes the standard normal cumulative density function.

The inefficiency $\text{IF}_{\bar{\pi}}(\sigma^2, \rho)$ can be computed accurately using one-dimensional numerical integration as $\bar{\pi}(z|\theta) \sim \mathcal{N}(\sigma^2/2, \sigma^2)$. We end this section by presenting an alternative set of more restrictive assumptions implying Part (i) of Assumption S3 and the proposal in Part (ii) of Assumption S3, i.e. (S2.4). This assumption provides greater understanding of the results above.

Assumption S4. *If $U_i \sim p_U(\cdot)$, $i = 1, \dots, G$, then the distribution of $\tilde{Z}_i(\theta, U_i)$ conditional on θ is $\mathcal{N}(-\sigma^2/2G, \sigma^2/G)$ with $\sigma^2 := \text{V}_{u \sim p_U}[Z]$ for $Z = \sum_{i=1}^G \tilde{Z}_i(\theta, U_i)$, which is independent of θ .*

Lemma S6 then implies the desired result.

Lemma S6. *Suppose that Assumption S4 holds and let*

$$Z = \sum_{i=1}^G \tilde{Z}_i(\theta, U_i) \text{ and } Z' = \sum_{i \neq j, i=1}^G \tilde{Z}_i(\theta', U_i) + \tilde{Z}_j(\theta', U'_j),$$

with $U_i \sim \bar{\pi}$ and $U'_j \sim p_{U_j}(\cdot)$. Then,

$$(S2.6) \quad \begin{bmatrix} z \\ z' \end{bmatrix} \sim \mathcal{N}\left(\begin{bmatrix} \frac{\sigma^2}{2} \\ -\frac{\sigma^2}{2}(1 - 2\rho) \end{bmatrix}, \sigma^2 \begin{bmatrix} 1 & \rho \\ \rho & 1 \end{bmatrix}\right), \text{ with } \rho = 1 - \frac{1}{G}.$$

S3. OPTIMAL TUNING - GENERAL CASE

Algorithm 2 assumes $m = 30$ so that \hat{d}_m can be assumed to be normal and the optimal λ can be computed easily. Section 4.3 argues that this can be suboptimal. We therefore

consider an alternative approach, based on assuming that \widehat{d}_m is a mixture of normals, which makes the tuning general since a mixture of normals with enough mixture components can approximate any distribution. We propose fitting a mixture of normals to \widehat{d}_m using characteristic functions.

The following lemma generalizes Lemma 2; its proof is in Section S8. The notation $\text{Mix-}\mathcal{N}(\mu, \sigma^2, \omega)$ means that we have a standardized finite mixture with C components. Its parameters are $\mu := \mu_{1:C}$, $\sigma := \sigma_{1:C}^2$, $\omega := \omega_{1:C}$ with $\sum_j \omega_j = 1$ and, by standardization, its mean and variance are $\sum_j \omega_j \mu_j = 0$ and $\sum_j \omega_j (\sigma_j^2 + \mu_j^2) - 1 = 1$.

Lemma S7. *Let $\bar{d}_m^{(h,l)} = \sqrt{\frac{m}{\gamma}}(\widehat{d}_m^{(h,l)} - d) \stackrel{iid}{\sim} \text{Mix-}\mathcal{N}(\mu, \sigma^2, \omega)$ follow mixture of normals for all h and l such that $\mathbb{E}[\bar{d}_m^{(h,l)}] = 0$ and $\mathbb{V}[\bar{d}_m^{(h,l)}] = 1$. The variance of $\log|\widehat{L}_B|$ when $a = d - \lambda$ is then*

$$\mathbb{V} \left[\log |\widehat{L}_B| \right] = \lambda \sum_{c=1}^C \omega_c (\nu_c^2 + (\eta_c - \eta)^2) + \lambda \eta^2,$$

where

$$\eta_c = \log \left(\frac{\sigma_c}{\lambda} \sqrt{\frac{\gamma}{m}} \right) + \frac{1}{2} (\log 2 + \mathbb{E}_{J_c} [\psi^{(0)}(1/2 + J_c)]),$$

$\eta = \sum_{c=1}^C \omega_c \eta_c$ and

$$\nu_c^2 := \frac{1}{4} (\mathbb{E}_{J_c} [\psi^{(1)}(1/2 + J_c)] + \mathbb{V}_{J_c} [\psi^{(0)}(1/2 + J_c)])$$

with $J_c \sim \text{Pois} \left(\frac{(\mu_c + \sqrt{\frac{m}{\gamma}} \lambda)^2}{2\sigma_c^2} \right)$ and $\psi^{(q)}$ is the polygamma function of order q . Furthermore,

$\mathbb{V} \left[\log |\widehat{L}_B| \right] < \infty$ for all $m > 0$, $\lambda > 0$ and μ, σ, ω .

Given the finite mixture distribution for \widehat{d}_m , it is straightforward to compute the probability that the estimator is positive, as this becomes a mixture of normal cumulative distribution functions. We can numerically evaluate the CT in (4.9) for the finite mixture of normals case, and can optimize λ for a given m . Figure S5 compares λ_{opt} from the mixture of normal approach to the simpler approach in Algorithm 2 where the d_k follow a Student t distribution with 4 degrees of freedom. The figure illustrates that when $m = 30$ (and above) the two

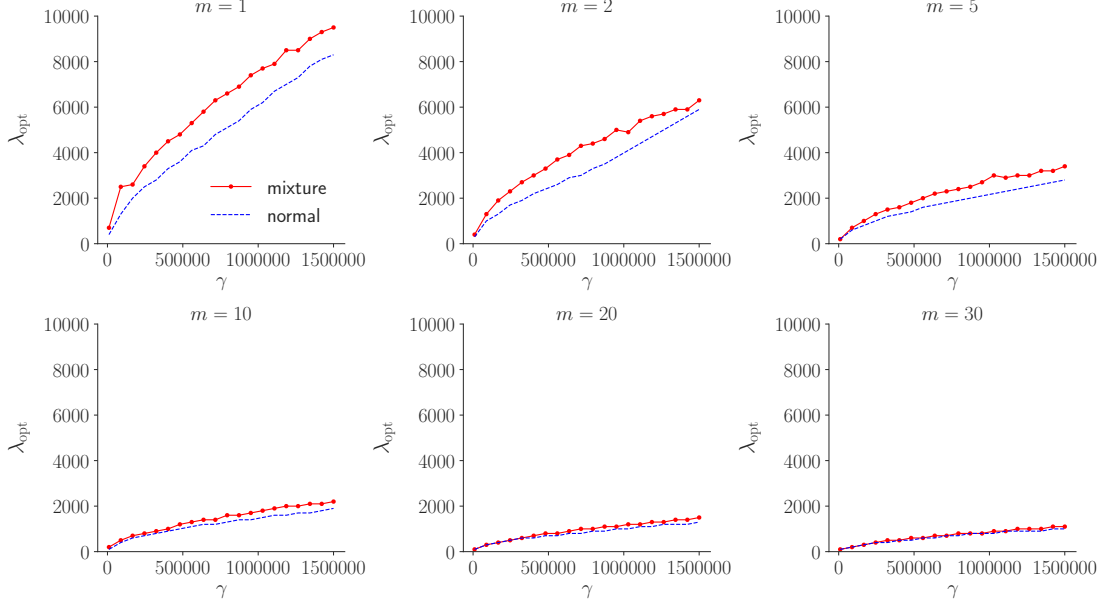


FIGURE S5. Optimal λ as a function of γ for the normal approach vs the finite mixture of normal approach. Each figure shows, for a specific value of m (see title of each panel), the λ obtained by minimizing the CT in (4.9) under a normal assumption for \hat{d}_m (blue dashed line) and a finite mixture of normal assumption for \hat{d}_m (red solid line).

approaches result in nearly indistinguishable optimal values for all γ ; when m is small, the optimal guidelines can differ substantially, especially for larger values of γ .

We now outline how to find the parameters $(\omega_{1:G}, \sigma_{1:G}^2, \mu_{1:G})$ in the finite mixture distribution. Let $X_1, \dots, X_n | \theta \stackrel{iid}{\sim} f_X(x|\theta)$ with a finite mean μ and variance σ^2 . We are interested in approximating the distribution of the sample mean $\bar{X}_n = n^{-1} \sum_{i=1}^n X_i$ by a mixture of normals

$$f_{\bar{X}_n}(x) \approx g_{\bar{X}_n}(x|\eta, \psi^2, \omega) = \sum_{c=1}^C \omega_c \mathcal{N}(x|\eta_c, \psi_c^2),$$

where $\mathcal{N}(x|\eta, \psi^2)$ denotes a normal density with mean η and variance ψ^2 . Let $\beta = \{\omega, \eta, \psi\}$ denote all the parameters of the mixture, and let $g_{\bar{X}_n}^{(\beta)}(x)$ denote the density for the sample mean from the mixture with parameters β .

The aim is to find the necessary number of mixture components C and the parameters β of the mixture that approximates $f_{\bar{X}_n}(x)$ well. We will do so by minimizing the L_2 distance

between $f_{\bar{X}_n}(x)$ and $g(x|\theta, \psi^2, \omega)$

$$d\left(f_{\bar{X}_n}, g_{\bar{X}_n}^{(\beta)}\right) = \int \left(f_{\bar{X}_n}(x) - g_{\bar{X}_n}^{(\beta)}(x)\right)^2 dx.$$

The L_2 distance is very convenient since by Plancherel's theorem we can turn the density matching problem into a Characteristic Function (CF) matching problem,

$$d\left(f_{\bar{X}_n}, g_{\bar{X}_n}^{(\beta)}\right) = \int \left(f_{\bar{X}_n}(x) - g_{\bar{X}_n}^{(\beta)}(x)\right)^2 dx = \int \left(\varphi_{\bar{X}_n}(t) - \varphi_{\bar{X}_n}^{(\beta)}(t)\right)^2 dt = d\left(\varphi_{\bar{X}_n}(t), \varphi_{\bar{X}_n}^{(\beta)}(t)\right),$$

where $\varphi_X(t)$ is the characteristic function $\varphi_X(t) := \mathbb{E}[e^{itX}]$ for a random variable X . Matching CFs is especially attractive here since the density of the sample mean $f_{\bar{X}_n}$ may be intractable, but its CF is straightforward to obtain,

$$\varphi_{\bar{X}_n}(t) = (\varphi_X(t/n))^n,$$

with $\varphi_X(t)$ the CF of $f_X(x|\theta)$. We will match CFs for the standardized mean $\bar{Z}_n = (\sqrt{n}/\sigma)(\bar{X}_n - \mu)$. Using the property $\varphi_{a+bX}(t) = e^{ita}\varphi_X(bt)$, we obtain the CF for the standardized mean as

$$\varphi_{\bar{Z}_n}(t) = e^{-it\mu\sqrt{n}/\sigma} (\varphi_X(t/(\sqrt{n}\sigma)))^n.$$

The CF for a normal mixture $\sum_{c=1}^C \omega_c \mathcal{N}(x|\eta_c, \psi_c^2)$ is $\varphi_X(t) = \sum_{c=1}^C \omega_c \varphi_{X_c}(t)$, where $\varphi_{X_c}(t) = \exp(i\eta_c t - \psi_c^2 t^2/2)$ is the CF of the c th mixture component.

We minimize $d\left(\varphi_{\bar{Z}_n}(t), \varphi_{\bar{Z}_n}^{(\beta)}(t)\right)$ with respect to β for a given C by reparameterizing the standard deviations in the mixture components in exponential form and the weights ω using the softmax function. The minimization is subject to the restrictions that the mixture has zero mean and unit variance: $\sum_{c=1}^C \omega_c \eta_c = 0$ and $\sum_{c=1}^C \omega_c (\kappa_c^2 + (\eta_c - \eta)^2) = 1$. These restrictions can be enforced directly or indirectly via penalties.

S4. EXACT VS APPROXIMATE SUBSAMPLING MCMC

Quiroz et al. (2019) propose a framework for subsampling MCMC using the bias-corrected likelihood estimator,

$$\widehat{L}_A := \exp\left(q + \widehat{d}_M - \frac{n^2}{2M} \widehat{\sigma}_{d_{u_i}}^2\right),$$

based on a subsample of size M . The bias-correction is only approximate so the pseudo-marginal sampler in Quiroz et al. (2019) targets a perturbed posterior which is within $O(n^{-1}M^{-2})$ from the true posterior in total variation distance. Thus, unlike the current exact approach, the posterior moments from the sampler in Quiroz et al. (2019) are only approximate. We can show that if the d_k are normally distributed, then

$$\sigma_{\log \widehat{L}_A}^2 := V[\log \widehat{L}_A] = \frac{\gamma}{M} + \frac{\gamma^2}{2M^3},$$

and we can then define the computational time

$$\text{CT}_A(M|\gamma, \rho = 0.99) = M \cdot \text{IF}\left(\sigma_{\log \widehat{L}_A}^2(M|\gamma, \rho = 0.99)\right).$$

Similarly to the block-Poisson estimator in Section 4.3, we can minimize this CT with respect to M , for each γ . The Relative Computational Time (RCT) of the optimal exact method proposed here against the approx in Quiroz et al. (2019) is

$$(S4.1) \quad \text{RCT}_{\text{opt}}(\gamma) = \frac{\text{CT}_E(\lambda_{\text{opt}}|\gamma, m, \rho = 0.99)}{\text{CT}_A(M_{\text{opt}}|\gamma, \rho = 0.99)}.$$

Figure S6 plots $\text{RCT}_{\text{opt}}(\gamma)$ as a function of γ for several values of m and shows that the approximate approach has lower CT, by a factor between 2 and 9 for $m = 30$, depending of the value of γ ; thus there is a trade-off between exactness and computational cost.

S5. TESTING THE ROBUSTNESS OF THE TUNING GUIDELINES

We now test the accuracy of the guidelines for tuning λ when $m = 30$. In particular, we will test the robustness of the guidelines to deviations from the main assumption behind the

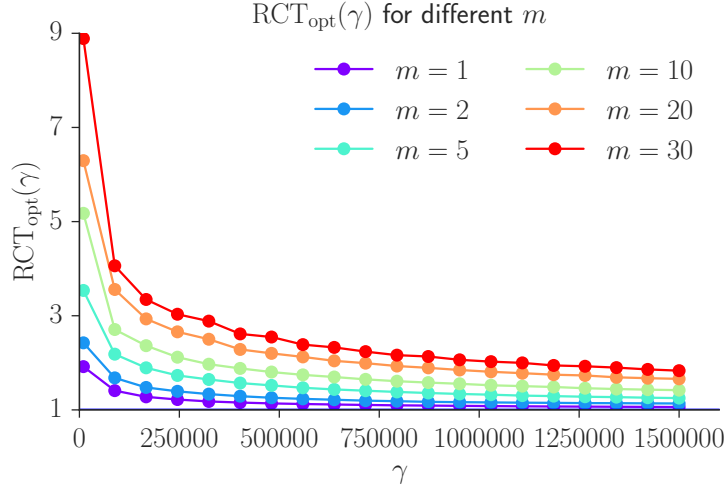


FIGURE S6. RCT in (S4.1) as a function of λ for different values of m .

derivation of the guidelines, i.e. $\gamma = n^2\sigma_d^2$ is independent of θ . To do so, we construct the differences $d_k = \ell_k - q_k$ in the following two ways:

- (1) *Correct assumption:* We sample a population d_k that does not depend on θ and obtain $\sigma_d^2 = V[d_k] = 1/n \sum_{k=1}^n (d_k - \bar{d})^2$.
- (2) *Incorrect assumption:* For each θ , we compute $d_k(\theta) = \ell_k(\theta) - q_k(\theta)$, taking $q_k(\theta)$ to be the data expanded control variate in Section 3.2. We then compute $\gamma(\theta) = n^2\sigma_d^2(\theta)$; in this setting, γ depends on θ and therefore violates the main assumption in the optimal tuning derivation.

The guidelines are tested as follows. We consider a simple Poisson regression model with one covariate and no intercept, $y_k \sim \text{Poisson}(\exp(\theta x_k))$. To make the experiment as clean as possible we choose a perfect proposal by computing $\bar{\pi}(\theta) \propto \int |\hat{L}(\theta, u)| p_U(u) du$ on a grid of θ values (by Monte Carlo simulation). Since θ is one dimensional, this distribution is easily sampled by the inverse cdf method. For each λ , we can now compute the empirical version of the CT in Section 5 by estimating the integrated auto-correlation time of $s\theta$ from a long MCMC chain for θ . Repeating this procedure for each λ on a grid we can select the λ that minimizes the empirical CT and compare it to λ_{opt} from Algorithm 2.

Figure S7 shows that when the λ_{opt} provided by the guidelines does not agree with the empirically obtained one, the difference in computational time between the different λ is

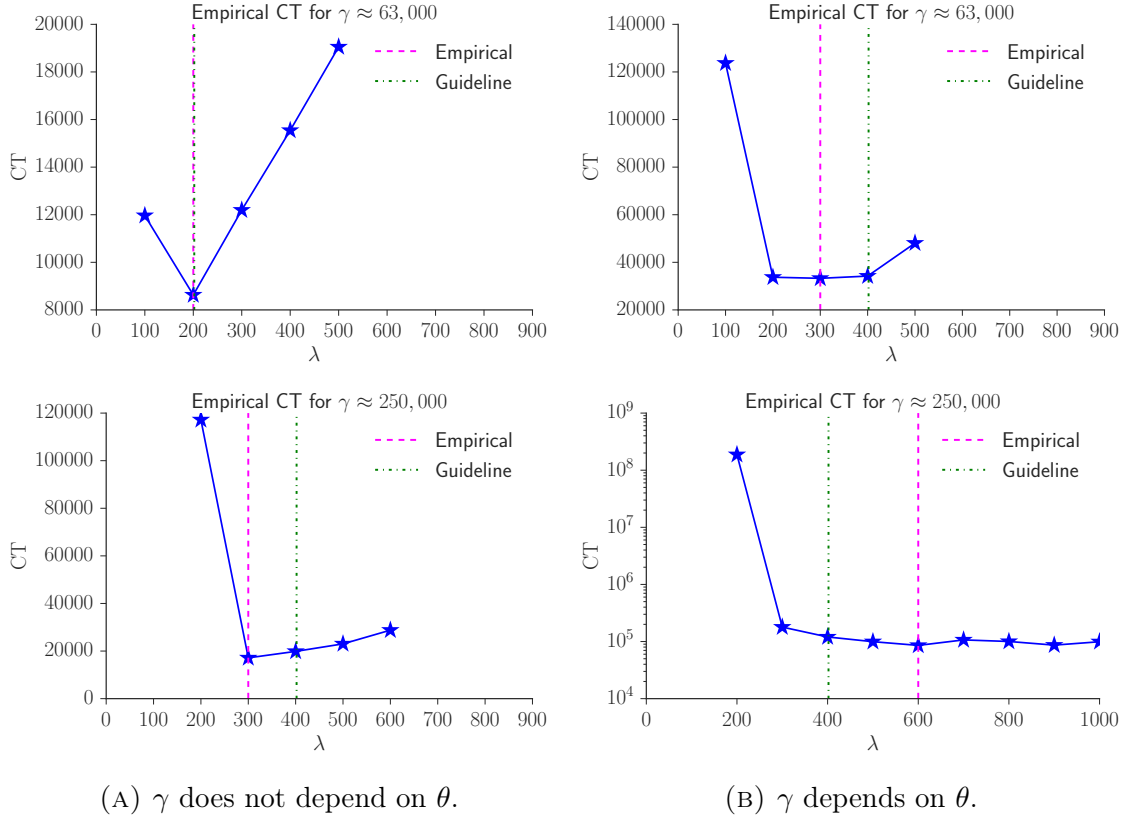


FIGURE S7. Testing the robustness of the tuning guidelines in Algorithm 2. Panels (A) show the empirical CT for two different γ values, when the assumption that γ is independent of θ is correct. Panels (B) show the empirical CT for two different γ values, but in a setting that violates the assumption that γ depends not depend on θ . The vertical lines correspond to the optimal λ according to the guidelines in Algorithm 2 (dotted green) and the empirically observed optimum (dashed magenta).

very small. We therefore conclude that the guidelines are sensible, and more importantly, they never suggest a λ which is too small resulting in a catastrophically large CT.

S6. THE BLOCK PMMH WITH $\widehat{L} \geq 0$

This section derives a special case of our algorithm in which the sign is 1 $\bar{\pi}$ -almost surely, which we refer to as the block PMMH. We provide guidelines for its optimal tuning.

S6.1. Convergence of the block PMMH. Suppose that the $\widehat{L}^{(i)}(\theta, u) \geq 0, i = 1, \dots, G$ for all $\theta \in \Theta, u_{1:G} \in \mathcal{U}^G$, so that the likelihood estimator is $\bar{\pi}$ -almost surely positive, i.e. $\Pr_{\bar{\pi}}(S = 1) = 1$. Then, $\bar{\pi}(d\theta) = \pi(d\theta)$ (the posterior), $C(\theta) = L(\theta)$ (the likelihood),

$\bar{C} = p(y)$ (the marginal likelihood), (4.7) becomes

$$\bar{\pi}(d\theta, du_{1:G}) = \frac{p_{\Theta}(d\theta)}{\bar{C}} \prod_{i=1}^G \hat{L}^{(i)}(\theta, u_i) p_U(du_i),$$

and (4.5) becomes

$$(S6.1) \quad \hat{E}_{\pi}[\psi] = \frac{1}{N} \sum_{i=1}^N \psi(\theta^{(i)}).$$

Then the following convergence result holds. Its proof follows from the proof of Theorem S1.

Corollary 1. *Suppose that $\hat{L}(\theta, u) \geq 0$, and that the Markov chain in Algorithm S2 is irreducible and aperiodic. Then,*

- (i) *Algorithm S1 is reversible.*
- (ii) *Algorithm S1 converges to $\bar{\pi}$ in total variation norm, with marginal $\pi(d\theta) = \int_{\mathcal{U}} \bar{\pi}(d\theta, du)$.*
- (iii) *Suppose that $E_{\pi}[|\psi|] < \infty$. Then, $\hat{E}_{\pi}[\psi] \rightarrow E_{\pi}[\psi]$ a.s. ($\bar{\pi}$).*
- (iv) *Define*

$$\text{IF}_{\bar{\pi}, \psi} = \frac{V_{\bar{\pi}}(\psi) + 2 \sum_{j=1}^{\infty} \bar{\Gamma}_j}{V_{\bar{\pi}}(\psi)},$$

where $\bar{\Gamma} = \text{Cov}_{\bar{\pi}}(\psi(\theta_0), \psi(\theta_j))$ and $(\theta_0, \dots, \theta_j, \dots)$ are the MCMC iterates of θ . If $V_{\bar{\pi}}[\psi] \text{IF}_{\bar{\pi}, \psi} = V_{\pi}[\psi] \text{IF}_{\bar{\pi}, \psi} < \infty$, then

$$\sqrt{N} \left(\hat{E}_{\pi}(\psi) - E_{\pi}(\psi) \right) \rightarrow \mathcal{N} \left(0, V_{\pi}(\psi) \text{IF}_{\bar{\pi}, \psi} \right).$$

We call the algorithm with a nonnegative likelihood estimator in Corollary 1 the block PMMH. By Part (ii) of Corollary 1, unlike the signed block PMMH, the iterates of θ for the block PMMH are distributed according to $\pi(d\theta)$.

S6.2. Tuning the block PMMH. We now consider tuning the block PMMH, which is a special case of the signed block PMMH with only positive signs and therefore $\tau := 1$; see Section 4.1.

Pitt et al. (2012) show that the optimal number of particles m , when $\sigma_{\log \hat{L}}^2 \propto 1/m$, is given implicitly by the $\sigma_{\log \hat{L}}^2$ that minimizes the computational time

$$(S6.2) \quad \text{CT}(\sigma_{\log \hat{L}}^2) := m \cdot \text{IF}(\sigma_{\log \hat{L}}^2) \propto \frac{\text{IF}(\sigma_{\log \hat{L}}^2)}{\sigma_{\log \hat{L}}^2},$$

where IF denotes the inefficiency factor of the pseudo-marginal chain; see also Doucet et al. (2015). This computational time only depends on $\sigma_{\log \hat{L}}^2$, which in turn is proportional to $1/m$, hence simplifying the expression compared to (4.9). Pitt et al. (2012) derive, based on several assumptions which we also invoke in Section S2, an analytic expression for the IF and shows that $\text{CT}(\sigma_{\log \hat{L}}^2)$ in (S6.2) is minimized when $\sigma_{\log \hat{L}}^2 \approx 1$. Under less restrictive assumptions Doucet et al. (2015); Sherlock et al. (2015) show that the optimal value of $\sigma_{\log \hat{L}}^2$ ranges between approximately 1 and 3.3.

The next lemma obtains the optimal $\sigma_{\log \hat{L}}^2$ for the block PMMH and is proved using the IF derived in Pitt et al. (2012), but incorporating our block scheme. The lemma shows that the block PMMH with $G = 100$ speeds up the independent pseudo-marginal significantly, as the optimal value of $\sigma_{\log \hat{L}}^2$ is 234, which is much larger than the recommended range 1 to 3.3 in Pitt et al. (2012).

Lemma S8. *Given the assumptions in Section S2, $\sigma_{\log \hat{L}}^2 \approx 2.16^2/(1 - \rho^2)$ minimizes (S6.2) when $\rho = 1 - 1/G$ is close to 1.*

S7. ADDITIONAL MATERIAL FOR THE EXPERIMENTS IN SECTION 5

Section 4.3 outlines a tuning strategy that requires determining the intrinsic variability of the control variates given by $\gamma(\theta) = n^2 \sigma_{d_{u_i}}^2$. Moreover, the tuning strategy requires \bar{d} to set the lower bound (see Step 4.), which is obtained by estimating $d(\theta)$. Figures S8 – S10 show how these quantities vary over the posterior draws for the three datasets used in Section 5.

Figures S11 – S13 illustrate the slow convergence of Firefly Monte Carlo for the θ_1 draws (the performance is similar for all parameters). A similar performance of Firefly Monte Carlo is reported by Bardenet et al. (2017); Quiroz et al. (2019); Li et al. (2020).

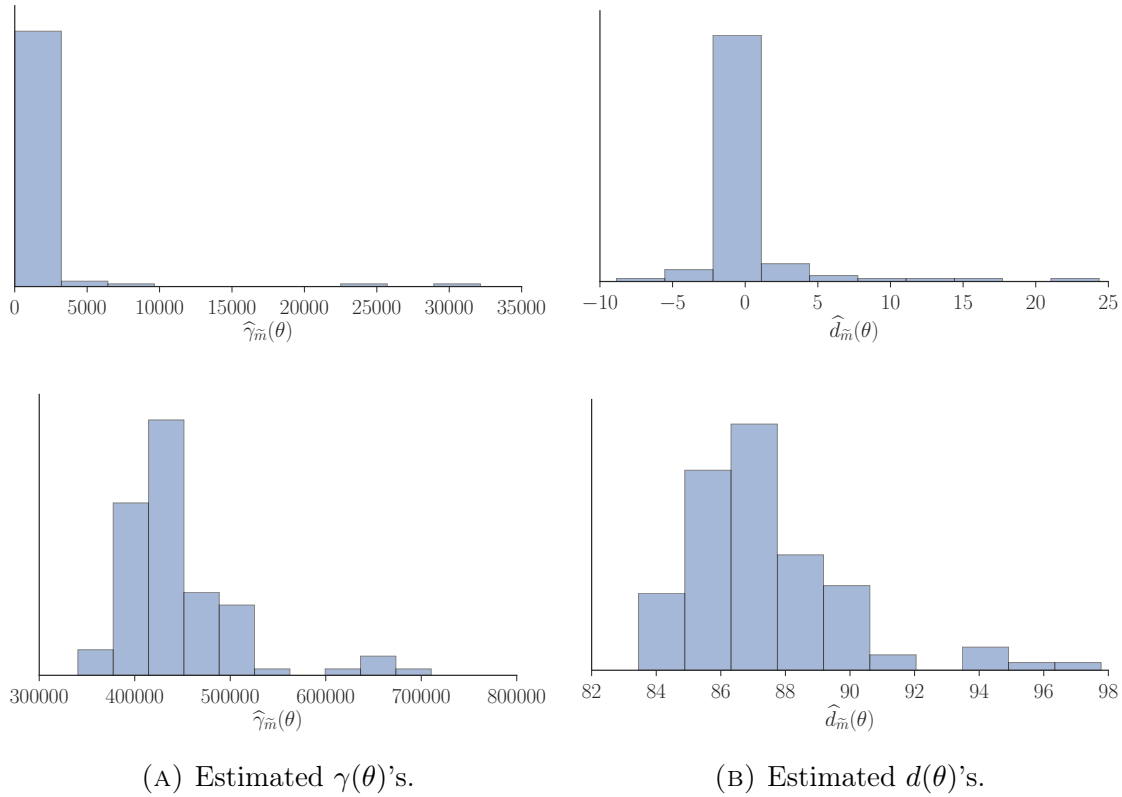


FIGURE S8. Estimating $\gamma(\theta)$ (left panel) and $d(\theta)$ (right panel) for different θ on the Covtype dataset. Estimates of $\gamma(\theta) = n^2 \sigma_{d_{u_i}}^2$ and $d(\theta)$ based on $\tilde{m} = 0.10n$ with parameter expanded control variates (top row) and data expanded control variates (bottom row). The histograms are obtained by (for a fixed u) estimating the quantities unbiasedly for 100 values of θ sampled from a multivariate Student t approximation of the posterior with 5 degrees of freedom. This generates over-dispersed θ values and hence a γ_{\max} which is conservative. Note that this figure is not useful for evaluating the normality assumption of $\hat{d}_{\tilde{m}}$, because u is fixed.

S8. PROOFS

S8.1. Proof of Lemma 1 . The estimator is given by (3.4); since the $\hat{d}_m^{(h,l)}$ are independent for all h and l , it follows that $\xi_1, \dots, \xi_\lambda$ are independent. The following lemma, whose proof is straightforward, is useful for the proof.

Lemma S9. *Suppose that $X \sim \text{Pois}(1)$ and that $A < \infty$. Then*

- (i) $E_X[A^X] = \exp(A - 1)$.
- (ii) $V_X[A^X] = \exp(-1) (\exp(A^2) - \exp(2A - 1))$.

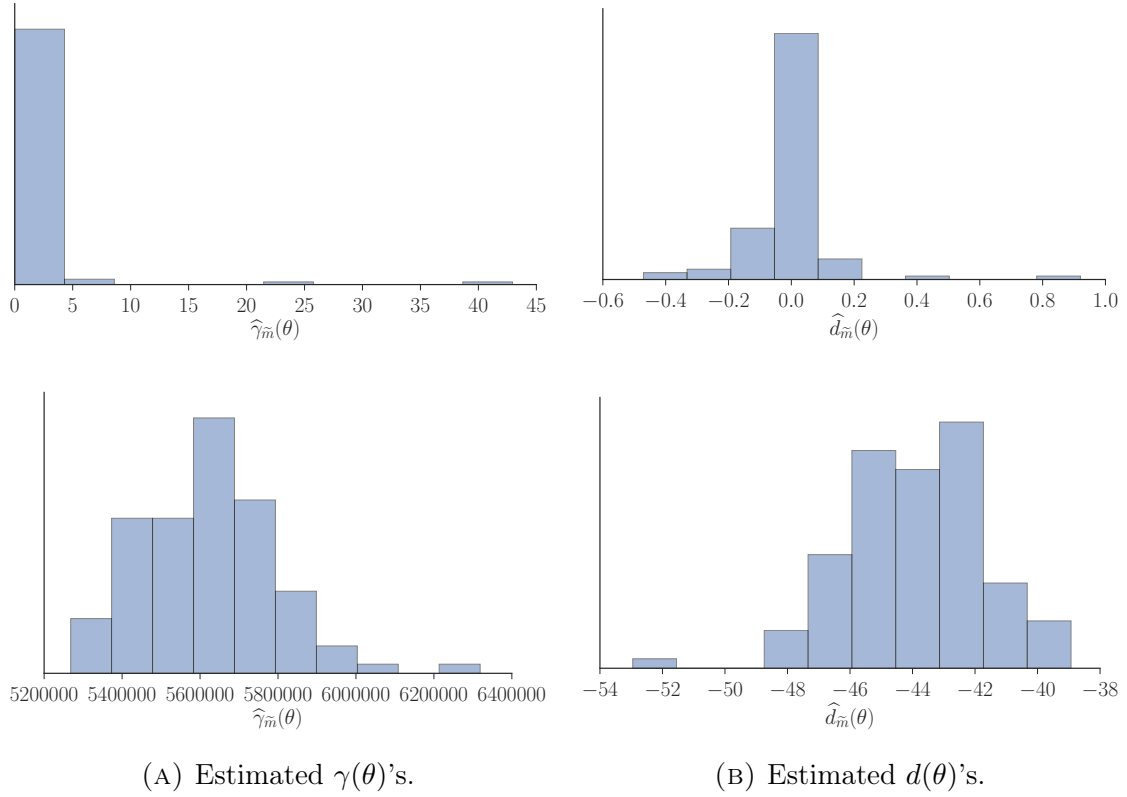


FIGURE S9. Estimating $\gamma(\theta)$ (left panel) and $d(\theta)$ (right panel) for different θ on the bankruptcy dataset. Estimates of $\gamma(\theta) = n^2 \sigma_{d_{u_i}}^2$ and $d(\theta)$ based on $\tilde{m} = 0.10n$ using parameter expanded control variates (top row) and data expanded control variates (bottom row). The histograms are obtained by, for a fixed u , estimating the quantities unbiasedly for 100 values of θ sampled from a multivariate Student t approximation of the posterior with 5 degrees of freedom. This generates over-dispersed θ values and hence we obtain a conservative γ_{\max} . This figure is not useful for evaluating the normality assumption of $\hat{d}_{\tilde{m}}$, because u is fixed.

Proof of Lemma 1. Proof of Part (i). By the law of iterated expectations,

$$\begin{aligned} \mathbb{E}[\xi] &= \mathbb{E}_{\mathcal{X}}[\mathbb{E}_{\hat{d}|\mathcal{X}}[\xi|\mathcal{X}]] = \exp(a/\lambda + 1) \mathbb{E}_{\mathcal{X}} \left[\left(\frac{d-a}{\lambda} \right)^{\mathcal{X}} \right] \\ &= \exp(d/\lambda), \end{aligned}$$

where the last equality follows from part (i) of Lemma S9. Since the ξ_l are independent for $l = 1, \dots, \lambda$,

$$\mathbb{E}[\widehat{L}_B] = \exp(q) \prod_{l=1}^{\lambda} \mathbb{E}[\xi_l] = \exp(q + d) = L.$$

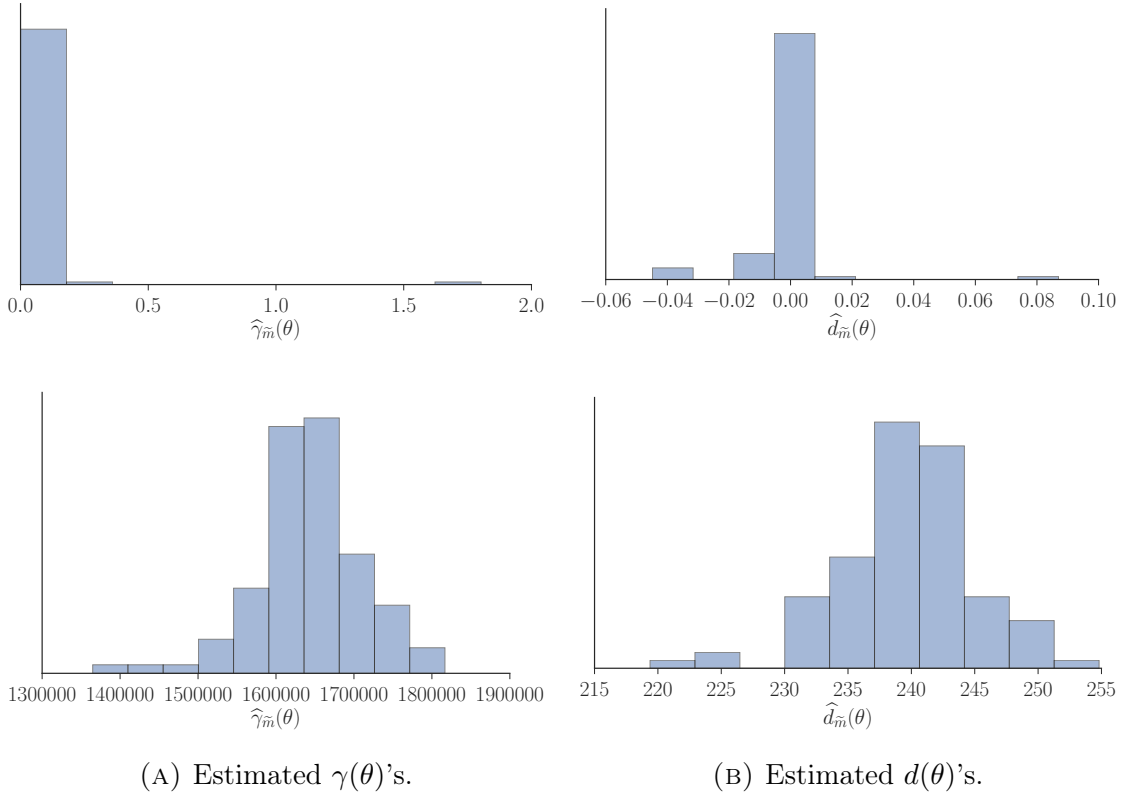


FIGURE S10. Estimating $\gamma(\theta)$ (left panel) and $d(\theta)$ (right panel) for different θ on the HIGGS dataset. Estimates of $\gamma(\theta) = n^2\sigma_{d_{u_i}}^2$ and $d(\theta)$ based on $\tilde{m} = 0.10n$ for parameter expanded control variates (top row) and data expanded control variates (bottom row). The histograms are obtained by (for a fixed u) estimating the quantities unbiasedly for 100 values of θ sampled from a multivariate Student t approximation of the posterior with 5 degrees of freedom. This generates over-dispersed θ values and hence we obtain a γ_{\max} which is conservative. Note that this figure is not useful for evaluating the normality assumption of $\hat{d}_{\tilde{m}}$, because u is fixed.

Proof of Part (ii) By (3.4), $\{\hat{d}_m^{(h,l)} \geq a, \forall h, l\} \subset \{\hat{L}_B \geq 0\}$. Hence

$$\Pr(\hat{L}_B \geq 0) \geq \Pr(\hat{d}_m^{(h,l)} \geq a, \text{ for all } h, l) = 1.$$

Proof of Part (iii) Since $\mathbb{E}[|\hat{L}_B|] \geq \left| \mathbb{E}[\hat{L}_B] \right|$ we obtain

$$\begin{aligned} \mathbb{V}[|\hat{L}_B|] &= \mathbb{E}[|\hat{L}_B|^2] - \mathbb{E}[|\hat{L}_B|]^2 \\ &\leq \mathbb{E}[\hat{L}_B^2] - \mathbb{E}[\hat{L}_B]^2 \\ &= \mathbb{V}[\hat{L}_B]. \end{aligned}$$

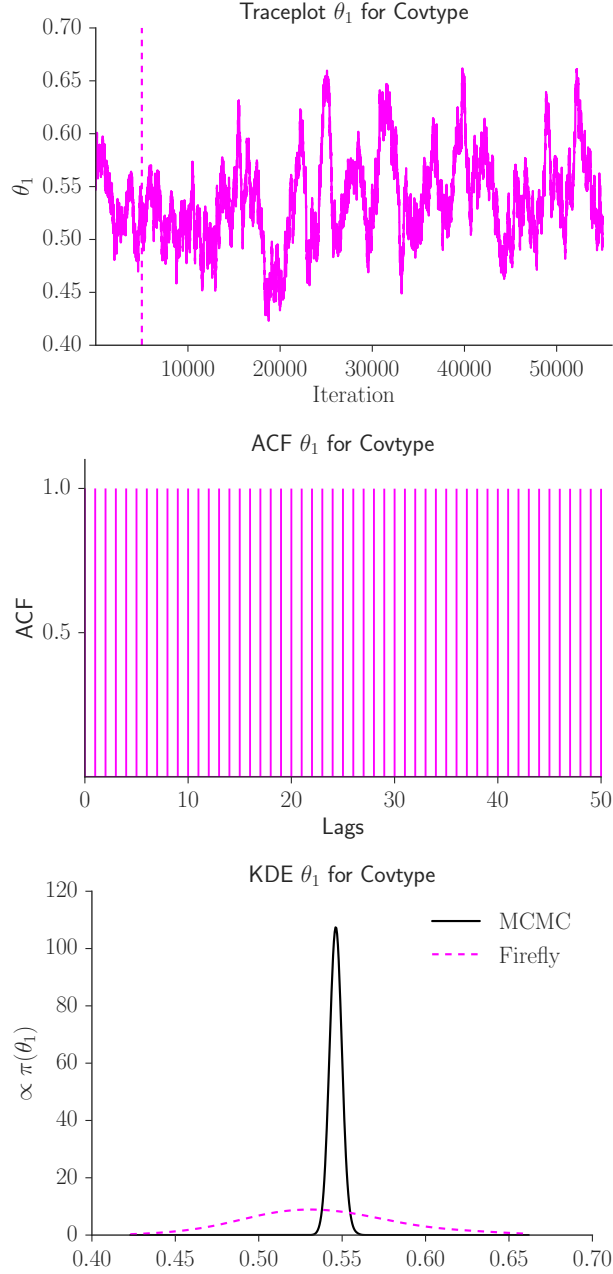


FIGURE S11. Results for Firefly Monte Carlo. Trace plots (upper panel), estimate of autocorrelation function (middle panel) and kernel density estimate (lower panel) of the posterior samples using FireFly Monte Carlo for the Covtype dataset. The vertical line in the upper panel marks the burn-in at iterate 5,000.

We now derive $V[\widehat{L}_B]$ and show that it is finite which proves the result. By the law of total variance

$$(S8.1) \quad V[\xi] = E_{\mathcal{X}}[V_{\widehat{d}|\mathcal{X}}[\xi|\mathcal{X}]] + V_{\mathcal{X}}[E_{\widehat{d}|\mathcal{X}}[\xi|\mathcal{X}]].$$

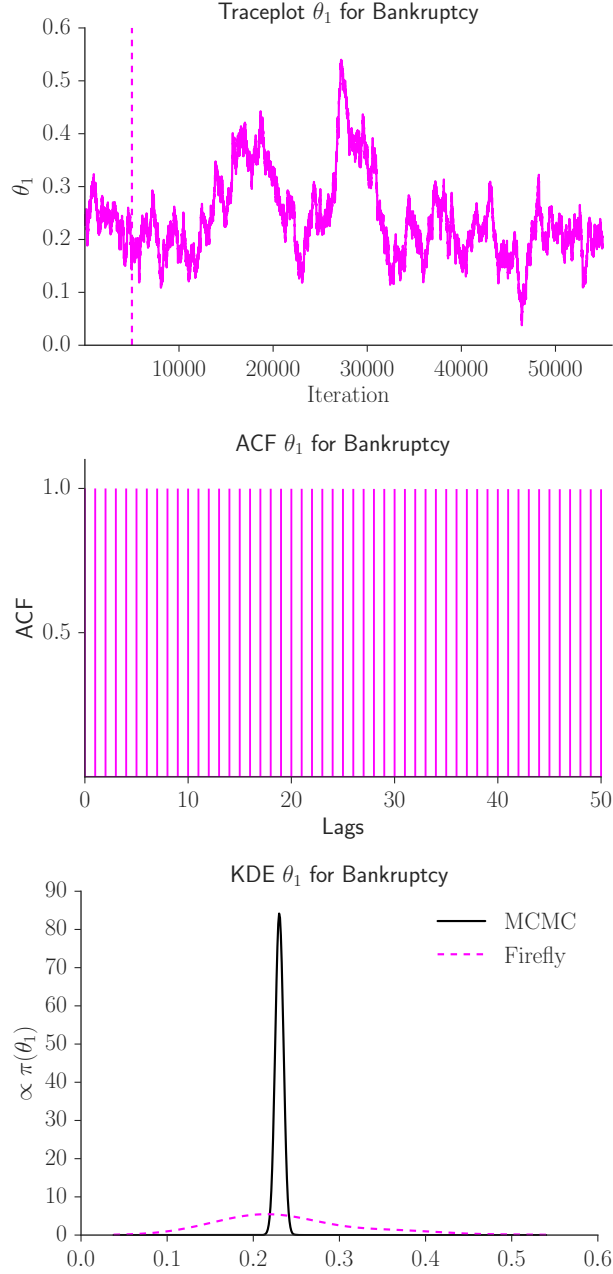


FIGURE S12. Results for Firefly Monte Carlo. Trace plots (upper panel), estimate of autocorrelation function (middle panel) and kernel density estimate (lower panel) of the posterior samples using FireFly Monte Carlo for the bankruptcy dataset. The vertical line in the upper panels marks the end of the burn-in period.

To compute $V_{\hat{d}|\mathcal{X}}[\xi|\mathcal{X}]$, note that for a collection of independent random variables X_1, \dots, X_J ,

$$(S8.2) \quad V \left[\prod_{j=1}^J X_j \right] = \prod_{j=1}^J (V[X_j] + E[X_j]^2) - \prod_{j=1}^J E[X_j]^2.$$

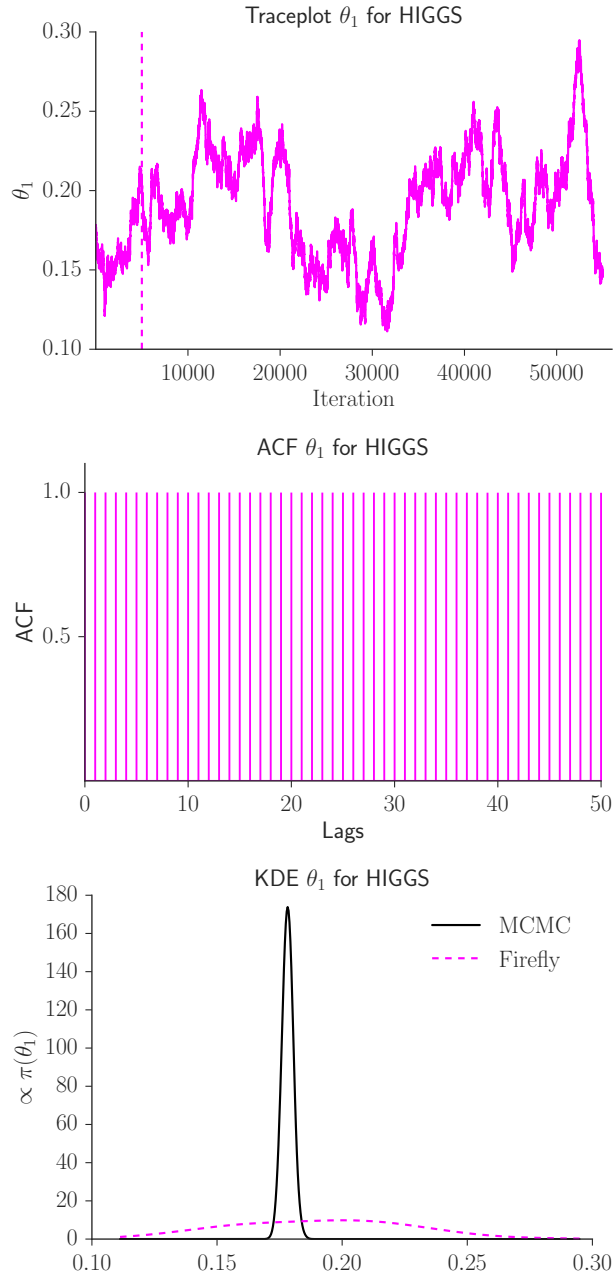


FIGURE S13. Results for Firefly Monte Carlo. Trace plots (upper panel), estimate of autocorrelation function (middle panel) and kernel density estimate (lower panel) of the posterior samples using FireFly Monte Carlo for the HIGGS dataset. The vertical line in the upper panels marks the burn-in 5,000.

Hence,

$$V_{\hat{a}|\mathcal{X}}[\xi|\mathcal{X}] = \exp\left(2\frac{a+\lambda}{\lambda}\right) \left(\left(\frac{\sigma_d^2}{\lambda^2} + \frac{(d-a)^2}{\lambda^2} \right)^x - \left(\frac{(d-a)^2}{\lambda^2} \right)^x \right)$$

and taking the outer expectations and applying Lemma S9,

$$\mathbb{E}_{\mathcal{X}}[\mathbb{V}_{\hat{a}|\mathcal{X}}[\xi|\mathcal{X}]] = \exp\left(\frac{2a}{\lambda} + \frac{(d-a)^2}{\lambda^2} + 1\right) \left(\exp\left(\frac{\sigma_d^2}{\lambda^2}\right) - 1\right).$$

Next,

$$\begin{aligned} \mathbb{V}_{\mathcal{X}}[\mathbb{E}_{\hat{a}|\mathcal{X}}[\xi|\mathcal{X}]] &= \exp\left(2\frac{a+\lambda}{\lambda}\right) \mathbb{V}_{\mathcal{X}}\left[\left(\frac{d-a}{\lambda}\right)^{\mathcal{X}}\right] \\ &= \exp\left(\frac{2a}{\lambda} + 1\right) \left(\exp\left(\frac{(d-a)^2}{\lambda^2}\right) - \exp\left(2\frac{d-a}{\lambda} - 1\right)\right), \end{aligned}$$

by part (ii) of Lemma S9 which, by (S8.1) and simplification, yields

$$\mathbb{V}[\xi] = \exp\left(\frac{1}{\lambda^2}(\sigma_d^2 + (d-a)^2) + \frac{2a}{\lambda} + 1\right) - \exp\left(\frac{2d}{\lambda}\right).$$

To compute $\mathbb{V}[\widehat{L}_B] = \exp(2q)\mathbb{V}\left[\prod_{l=1}^{\lambda} \xi_l\right]$, we use (S8.2) with $\mathbb{E}[\xi]^2 = \exp(2d/\lambda)$ to obtain

$$\begin{aligned} \mathbb{V}\left[\prod_{l=1}^{\lambda} \xi_l\right] &= \exp\left(\sum_{l=1}^{\lambda} \frac{1}{\lambda^2}(\sigma_d^2 + (d-a)^2) + \frac{2a}{\lambda} + 1\right) - \exp\left(\sum_{l=1}^{\lambda} \frac{2d}{\lambda}\right) \\ &= \exp\left(\frac{1}{\lambda}(\sigma_d^2 + (d-a)^2) + 2a + \lambda\right) - \exp(2d). \end{aligned}$$

This expression exists as long as $\sigma_d^2 < \infty$.

Proof of Part (iv). To minimize $\mathbb{V}[\widehat{L}_B]$ above for a fixed $\lambda > 0$, it is sufficient to minimize the exponent

$$f(a) = \frac{1}{\lambda}(\sigma_d^2 + (d-a)^2 + 2a + \lambda).$$

Since $f'(a) = -2(d-a)/\lambda + 2$ and $f''(a) = 2/\lambda > 0$, $a = d - \lambda$ is the minimum.

Proof of Part (v). This follows from the expression of the variance $\mathbb{V}[\widehat{L}_B]$ derived in the proof of part (iii) of Lemma 1 and that of (3.4) derived in Papaspiliopoulos (2009). \square

Proof of Lemma 2. The proof follows from the more general Lemma S7. \square

Proof of Lemma 3. Note that

$$\Pr(\widehat{L}_B \geq 0) = \Pr\left(\prod_{l=1}^{\lambda} \xi_l \geq 0\right)$$

and $\{\widehat{L}_B < 0\}$ can only occur if there is an odd number of negative terms ξ_l , $l = 1, \dots, \lambda$. (Feller, 2008, p. 277) gives an expression for the probability of an odd number of negatives terms among a total of λ terms that depends on the probability of a single ξ_l being negative, i.e. $\Pr(\xi_l < 0)$. From this we obtain

$$\Pr(\widehat{L}_B \geq 0) = \frac{1}{2} \left(1 + (1 - 2 \Pr(\xi_l < 0))^\lambda\right).$$

Notice that

$$\Pr(\xi_l < 0) = \sum_{j=1}^{\infty} \Pr\left(\prod_{l=1}^j A_m^{(l)} < 0\right) \Pr(\mathcal{X}_l = j), \quad \mathcal{X}_l \sim \text{Pois}(1),$$

and we can again apply the result in Feller (2008) to obtain

$$\Pr\left(\prod_{l=1}^j A_m^{(l)} < 0\right) = \frac{1}{2} \left(1 - (1 - 2 \Pr(\xi_l < 0))^j\right),$$

concluding the proof. □

Proof of Lemma S2. We need to show that $p_U(du)q_U(du'|u) = p_U(du')q_U(du|u')$. Now,

$$\begin{aligned} p_U(du)q_U(du'|u) &= \prod_{k=1}^G p_{U_k}(du_k) \frac{1}{G} \sum_{i=1}^G p_{U_i}(u_i) \prod_{j \neq i} \delta_{u_j}(du'_j) \\ &= \prod_{k=1}^G p_{U_k}(du'_k) \frac{1}{G} \sum_{i=1}^G p_{U_i}(u'_i) \prod_{j \neq i} \delta_{u'_j}(du_j) \end{aligned}$$

because $g(du')\delta_{u'}(du) = g(du)\delta_u(du')$ for any measure $g(\cdot)$. □

Proof of Theorem S1. Part (i). Reversibility follows because we are dealing with a MH sampler.

Part (ii). The proof is essentially that of Theorem 1 of Andrieu and Roberts (2009), but under slightly different conditions. Consider first the case $G = 1$. Let $\mathcal{B}(\Theta)$ be the Borel

sets of Θ and $\mathcal{B}(\mathcal{U})$ the Borel sets of \mathcal{U} . We will first show that if Algorithm S2 can reach the set $A \in \mathcal{B}(\Theta)$ from $\theta \in \Theta$ in one step, i.e. $P_\Theta(\theta; A) > 0$, then $\bar{P}_{\Theta,U}(\theta, u; A \times B) > 0$ for any $u \in \mathcal{U}$ and $B \in \mathcal{B}(\mathcal{U})$ with $P_U(B) > 0$, where $\bar{P}_{\Theta,U}$ is the transition kernel of Algorithm S1 and is given by

$$\bar{P}_{\Theta,U}(\theta, u; d\theta', du') = \bar{K}_{\Theta,U}(\theta, u; d\theta', du') + \delta_{\theta,u}(d\theta', du') \left(1 - \int \bar{K}_{\Theta,U}(\theta, u; d\theta', du') \right),$$

with $\bar{K}_{\Theta,U}(\theta, u; d\theta', du') = \alpha_{\Theta,U}(\theta, u, \theta', u') q_\Theta(\theta; d\theta') q_U(u; du')$.

Let $\alpha_Z(z, z') = 1 \wedge \exp(z' - z)$, where z and z' are defined in Section S2. We first note that $r_{\Theta,U}(\theta, u; \theta', u') = e^{z' - z} r_\Theta(\theta; \theta')$, and that $1 \wedge (xy) \geq (1 \wedge x)(1 \wedge y)$. Hence, $\alpha_{\Theta,U}(\theta, u, \theta', u') \geq \alpha_\Theta(\theta, \theta') \alpha_Z(z, z')$, so that $\bar{K}_{\Theta,U}(\theta, u; d\theta', du') \geq K_\Theta(\theta; d\theta') \alpha_Z(z, z') q_U(u; du')$ and that

$$\bar{P}_{\Theta,U}(\theta, u; d\theta', du') \geq \bar{K}_{\Theta,U}(\theta, u; d\theta', du').$$

Thus, if $\bar{P}_{\Theta,U}(\theta, u; A \times B) = 0$, then $K_\Theta(\theta; d\theta') \alpha_Z(z, z') q_U(u; du') = 0$ almost everywhere $\theta' \in A$ as $\alpha_Z(z, z') q_U(u; du') > 0$ by Part (i) of Assumption S1. But this contradicts Part (ii) of Assumption S1. This proves the one step result. Now we can similarly show by induction that if $P_\Theta^i(\theta; A) > 0$ for $i = 1, \dots, k$ implies that $\bar{P}_{\Theta,U}(\theta, u; A \times B) > 0$ for any $u \in \mathcal{U}$ and $B \in \mathcal{B}(\mathcal{U})$ with $P_U(B) > 0$, then the same holds true for $i = k + 1$. This completes the proof for $G = 1$.

We now consider the $G = 2$ case. We will show that for $k \geq 2$, if $P_\Theta^k(\theta; A) > 0$ then $\bar{P}_{\Theta,U}^k(\theta, u_{1:2}; A \times (B_1 \times B_2)) > 0$ for $u_{1:2} \in \bar{\mathcal{U}}^2$ with $p_U(B_1) > 0$ and $p_U(B_2) > 0$. Let $\tilde{B}_{-2} = B_1 \times \{u_2\}$ and $\tilde{B}_{-1} = \{u_1\} \times B_2$. Then, we can show similarly to the $G = 1$ case that if $P_\Theta(\theta; A) > 0$, then $\bar{P}_{\Theta,U}(\theta, u_{1:2}; A \times (\tilde{B}_{-1} \cup \tilde{B}_{-2})) > 0$. The result for $k \geq 2$ follows as in the $G = 1$ case.

We can similarly obtain the result for a general G . If $k \geq G$ and $P_\Theta^k(\theta; A) > 0$ then $\bar{P}_{\Theta,U}^k(\theta, u_{1:G}; A \times (B_1 \times B_2 \times \dots \times B_G)) > 0$, where $B_i \in \mathcal{B}(\mathcal{U})$ with $p_U(B_i) > 0$ for all $i = 1, \dots, G$. Suppose that the result is true for $G = 1, \dots, g$. Now define $\tilde{B}_{-i} = B_1 \times B_2 \times \dots \times B_{i-1} \times \{u_i\} \times B_{i+1} \times \dots \times B_{g+1}$. Then, by the induction hypothesis, if $P_\Theta^g(\theta; A) > 0$, then

$\bar{P}_{\Theta,U}^g(\theta, u_{1:g+1}; A \times (B_{-1} \cup \dots \cup B_{-g-1})) > 0$ assuming that $p_U(B_i) > 0$ for $i = 1, \dots, g+1$. The required result now follows as in the $G = 1$ case.

The irreducibility and aperiodicity of the sampling scheme now follows from that of Algorithm S2.

Part (iii) follows from the strong law of large numbers for Markov chain, see e.g. Meyn and Tweedie (2012, Theorem 17.0.1).

To prove Part (iv), we first consider the numerator of (4.5). By Theorem 27 in Roberts and Rosenthal (2004),

$$\sqrt{N} \left(N^{-1} \sum_{i=1}^N S_i \psi_i - E_{\bar{\pi}}(S\psi) \right) \rightarrow N \left(0, V_{\bar{\pi}}(\psi S) \text{IF}_{\bar{\pi}, \psi S} \right).$$

Next, by the strong law of large numbers for Markov chains $N^{-1} \sum_{i=1}^N S_i \rightarrow E_{\bar{\pi}}(S)$ $\bar{\pi}$ -almost surely, i.e. the denominator of (4.5) converges to $E_{\bar{\pi}}(S) \neq 0$. The result now follows from Slutsky's theorem. An alternative proof is given in Lyne et al. (2015) based on a bivariate CLT for the numerator and denominator of (4.5), followed by the delta method to prove the result. The delta method is valid under the assumption $E_{\bar{\pi}}(S) \neq 0$. \square

Proof of Lemma S1. Using the notation in (S2.1), it is straightforward to show that

$$\bar{\pi}(du_{1:G}|\theta) = \prod_{i=1}^G \exp\left(\tilde{z}_i(u_i, \theta)\right) p_{U_i}(u_i).$$

\square

S8.2. Proofs for Section S2.

Proof of Lemma S4. By Assumption S2 and $\bar{\pi}(d\theta, du) = \bar{\pi}(\theta)\bar{\pi}(du|\theta)$,

$$\bar{\pi}(\theta, dv, dz, dw) = \bar{\pi}(d\theta, du) |J(\theta, u)| = \exp(z) C(\theta) p(d\theta, dv, dz, dw).$$

Hence, $\bar{\pi}(d\theta, dv, dz) = \exp(z)C(\theta)p(d\theta, dv, dz)$ and

$$\begin{aligned}\bar{\pi}(d\theta, ds, dz) &= \exp(z)C(\theta) \int_{s=\text{sign}(v)} p(d\theta, dv, dz) \\ &= \exp(z)\bar{\pi}(\theta)p(ds|\theta)p(dz|\theta),\end{aligned}$$

with $p(ds|\theta) := \int_{s=\text{sign}(v)} p(dv|\theta)$. □

Proof of Lemma S5. Part (i) follows because

$$\frac{\bar{\pi}(d\theta', ds', dz')}{\bar{\pi}(d\theta, ds, dz)} \frac{\bar{\pi}(d\theta)p(ds|\theta)q(z'; dz|\sigma^2, \rho)}{\bar{\pi}(d\theta')p(ds'|\theta')q(z; dz'|\sigma^2, \rho)},$$

where the perfect proposals for θ and s cancel the corresponding terms in $\bar{\pi}$. Moreover, we can show that

$$p(dz)q(z; dz'|\sigma^2, \rho) = p(dz')q(z'; dz|\sigma^2, \rho).$$

Part (ii) follows from Part (i) and the fact that $q(z; dz'|\sigma^2, \rho)$ does not depend on θ and s . Part (iii) then follows from Lemma 4 in Pitt et al. (2012), but with the probability of accepting a proposal conditional on z which arises from the correlated proposal. □

Proof of Lemma S6. $E[Z'] = (G - 2)\sigma^2/2G$ since, under Assumption S4,

$$\sum_{i \neq j, i=1}^G Z_i(\theta', U_i) \sim \mathcal{N}\left(\frac{(G-1)\sigma^2}{2G}, \frac{(G-1)\sigma^2}{G}\right) \quad \text{and} \quad Z_j(\theta', U_j) \sim \mathcal{N}\left(-\frac{\sigma^2}{2G}, \frac{\sigma^2}{G}\right).$$

It also follows that $V[Z'] = \sigma^2$. Moreover, $Z \sim \mathcal{N}(\sigma^2/2, \sigma^2)$, concluding the proof. □

To prove Lemma S7, we first need the preliminary Lemmas S10 to S12.

Lemma S10. (Non-central χ^2 is a Poisson mixture of central χ^2). If $J \sim \text{Pois}(\mu/2)$ and $W|J \sim \chi^2(k + 2J)$, then marginally $W \sim \chi^2(k, \mu)$.

Proof. See Walck (1996). □

Lemma S11. (Moments of log central χ^2 . (Pav, 2015)). If $W \sim \chi^2(k)$ and $Y = \log W$, then $EY = \log 2 + \psi(k/2)$ and $VY = \psi^{(1)}(k/2)$.

Lemma S12. (Moments of log non-central χ^2). If $W \sim \chi^2(k, \mu)$ and $Y = \log W$, then

$$\begin{aligned} \mathbb{E}[Y] &= \log 2 + \mathbb{E}_J (\psi^{(0)}(k/2 + J)) \\ \mathbb{V}[Y] &= \mathbb{E}_J [\psi^{(1)}(k/2 + J)] + \mathbb{V}_J [\psi^{(0)}(k/2 + J)], \end{aligned}$$

where $J \sim \text{Pois}(\mu/2)$ and $\psi^{(q)}$ is the polygamma function of order q .

Proof. Follows from Pav (2015). From the mixture representation in Lemma S10 we know that we can represent $W \sim \chi^2(k, \mu)$ as $J \sim \text{Pois}(\mu/2)$ and $W|J \sim \chi^2(k + 2J)$. By the law of iterated expectations and Lemma S11

$$\mathbb{E}[Y] = \mathbb{E}_J[\mathbb{E}_{W|J}[Y]] = \log 2 + \mathbb{E}_J [\psi^{(0)}(k/2 + J)].$$

Also, from the law of total variance and Lemma S11

$$\mathbb{V}[Y] = \mathbb{E}_J[\mathbb{V}_{W|J}[Y]] + \mathbb{V}_J[\mathbb{E}_{W|J}[Y]] = \mathbb{E}_J [\psi^{(1)}(k/2 + J)] + \mathbb{V}_J [\psi^{(0)}(k/2 + J)].$$

□

Proof of Lemma S7. When $a = d - \lambda$ we have

$$\log |\widehat{L}_B| = q + d + \sum_{l=1}^{\lambda} \sum_{h=1}^{\mathcal{X}_l} \log \left(\left| \frac{\widehat{d}_m^{(h,l)} - d}{\lambda} + 1 \right| \right) = q + d + \sum_{l=1}^{\lambda} \sum_{h=1}^{\mathcal{X}_l} \log \left(\left| \frac{\sqrt{\frac{\gamma}{m}} \bar{d}_m^{(h,l)}}{\lambda} + 1 \right| \right),$$

where $\mathcal{X}_l \sim \text{Pois}(1)$, $l = 1, \dots, \lambda$. Let $I^{(h,l)} \in \{1, \dots, C\}$ be indicators such that $I^{(h,l)} = c$ means that observation $\bar{d}_m^{(h,l)}$ comes from the c th mixture component $\mathcal{N}(\mu_c, \sigma_c^2)$ with $\Pr(I^{(h,l)} = c) = \omega_c$. Now, since the $\bar{d}_m^{(h,l)}$ are *iid* and the total number of $\bar{d}_m^{(h,l)}$ is $\sum_{l=1}^{\lambda} \mathcal{X}_l$ we have

$$\mathbb{V} \left(\log |\widehat{L}_B| \mid \mathcal{X}_{1:\lambda} \right) = \left(\sum_{l=1}^{\lambda} \mathcal{X}_l \right) \mathbb{V} \log \left(\left| \frac{\sqrt{\frac{\gamma}{m}} \bar{d}_m^{(h,l)}}{\lambda} + 1 \right| \right).$$

Define

$$X^{(h,l)} = \frac{\sqrt{\frac{\gamma}{m}} \left(\bar{d}_m^{(h,l)} - \mu_{I^{(h,l)}} \right)}{\lambda},$$

and note that

$$X^{(h,l)} \mid (I^{(h,l)} = c) \sim N(0, \tilde{\sigma}_c^2),$$

where $\tilde{\sigma}_c^2 = \frac{\sigma_c^2}{\lambda^2} \frac{\gamma}{m}$. Now, conditional on $I^{(h,l)} = c$, we have

$$\begin{aligned}
\log \left(\left| \frac{\sqrt{\frac{\gamma}{m}} \bar{d}_m^{(h,l)}}{\lambda} + 1 \right| \right) &= \log \left(\left| X^{(h,l)} + \frac{\sqrt{\frac{\gamma}{m}} \mu_c + \lambda}{\lambda} \right| \right) \\
&\stackrel{d}{=} \log \left(\left| \tilde{\sigma}_c Z + \frac{\sqrt{\frac{\gamma}{m}} \mu_c + \lambda}{\lambda} \right| \right), \text{ where } Z \sim \mathcal{N}(0, 1) \\
&= \log \tilde{\sigma}_c + \log \left(\left| Z + \frac{\sqrt{\frac{\gamma}{m}} \mu_c + \lambda}{\lambda \tilde{\sigma}_c} \right| \right) \\
&= \log \left(\frac{\sigma_c}{\lambda} \sqrt{\frac{\gamma}{m}} \right) + \log \left(\left| Z + \frac{\mu_c + \sqrt{\frac{m}{\gamma}} \lambda}{\sigma_c} \right| \right) \\
&= \log \left(\frac{\sigma_c}{\lambda} \sqrt{\frac{\gamma}{m}} \right) + \frac{1}{2} \log \left(\left(Z + \frac{\mu_c + \sqrt{\frac{m}{\gamma}} \lambda}{\sigma_c} \right)^2 \right) \\
&\stackrel{d}{=} \log \left(\frac{\sigma_c}{\lambda} \sqrt{\frac{\gamma}{m}} \right) + \frac{1}{2} \log (W^{(h,l)}), \\
&\text{where } W^{(h,l)} \sim \chi^2 \left(1, \frac{(\mu_c + \sqrt{\frac{m}{\gamma}} \lambda)^2}{\sigma_c^2} \right).
\end{aligned}$$

where $\chi^2(k, \lambda)$ denotes the non-central χ^2 distribution with k degrees of freedom and non-centrality parameter λ . So $\log \left(\left| \frac{\sqrt{\frac{\gamma}{m}} \bar{d}_m^{(h,l)}}{\lambda} + 1 \right| \right)$ is a mixture of log of non-central χ^2 variables with component means and variances given by Lemma S12

$$\eta_c := \mathbb{E} \log \left(\left| \frac{\sqrt{\frac{\gamma}{m}} \bar{d}_m^{(h,l)}}{\lambda} + 1 \right| \middle| I^{(k,l)} = c \right) = \log \left(\frac{\sigma_c}{\lambda} \sqrt{\frac{\gamma}{m}} \right) + \frac{1}{2} (\log 2 + \mathbb{E}_{J_c} (\psi^{(0)}(1/2 + J_c)))$$

and

$$\nu_c^2 := \mathbb{V} \log \left(\left| \frac{\sqrt{\frac{\gamma}{m}} \bar{d}_m^{(h,l)}}{\lambda} + 1 \right| \middle| I^{(k,l)} = c \right) = \frac{1}{4} [\mathbb{E}_{J_c} (\psi^{(1)}(1/2 + J_c)) + \mathbb{V}_{J_c} (\psi^{(0)}(1/2 + J_c))]$$

where the J_c are independent and $J_c \sim \text{Pois} \left(\frac{(\mu_c + \sqrt{\frac{m}{\gamma}} \lambda)^2}{2\sigma_c^2} \right)$. By the mean and variance of a finite mixture we then have

$$\begin{aligned} \eta &:= \mathbb{E} \log \left(\left| \frac{\sqrt{\frac{\gamma}{m}} \bar{d}_m^{(h,l)}}{\lambda} + 1 \right| \right) = \sum_{c=1}^C \omega_c \eta_c \\ \mathbb{V} \log \left(\left| \frac{\sqrt{\frac{\gamma}{m}} \bar{d}_m^{(h,l)}}{\lambda} + 1 \right| \right) &= \sum_{c=1}^C \omega_c (\nu_c^2 + (\eta_c - \eta)^2). \end{aligned}$$

Finally,

$$\begin{aligned} \mathbb{V} \left(\log \left| \widehat{L}_B \right| \right) &= \mathbb{E}_{\mathcal{X}_{1:\lambda}} \mathbb{V} \left(\log \left| \widehat{L}_B \right| \mid \mathcal{X}_{1:\lambda} \right) + \mathbb{V}_{\mathcal{X}_{1:\lambda}} \mathbb{E} \left(\log \left| \widehat{L}_B \right| \mid \mathcal{X}_{1:\lambda} \right) \\ &= \mathbb{E}_{\mathcal{X}_{1:\lambda}} \left[\left(\sum_{l=1}^{\lambda} \mathcal{X}_l \right) \sum_{c=1}^C \omega_c (\nu_c^2 + (\eta_c - \eta)^2) \right] + \mathbb{V}_{\mathcal{X}_{1:\lambda}} \left(\left(\sum_{l=1}^{\lambda} \mathcal{X}_l \right) \eta \right) \\ &= \lambda \sum_{c=1}^C \omega_c (\nu_c^2 + (\eta_c - \eta)^2) + \lambda \eta^2. \end{aligned}$$

$\mathbb{V} \left(\log \left| \widehat{L}_B \right| \right)$ is finite since $\psi^{(1)}(1/2 + J) \leq \pi^2/2$ for all $J \geq 0$ and for all $J \geq 0$

$$\left(\psi^{(0)}(1/2 + J) \right)^2 = \left(\psi^{(0)}(1) - 2 \log 2 + 2 \sum_{k=1}^J \frac{1}{2k-1} \right)^2 < \left(\psi^{(0)}(1) - 2 \log 2 + 2J \right)^2$$

and the Poisson has finite first and second moments. □

S8.3. Proofs for Section S6.

Proof of Lemma S8. The result follows from numerically optimizing the expression

$$\text{CT}(\sigma^2, \rho) := \frac{\text{IF}(\sigma^2, \rho)}{\sigma^2},$$

with IF defined in Part (iii) of (S5). □